UNIVERSITÄT PADERBORN
Die Universität der Informationsgesellschaft

Characterization Techniques of Solids

X-ray Diffraction of Solids and Semiconductors

D.J. As,

Universität Paderborn, Department Physik,
Warburger Str. 100,
33098 Paderborn, Germany
Raum P8.2.10
Tel. 05251 60 5838
E-mail: d.as@uni-paderborn.de

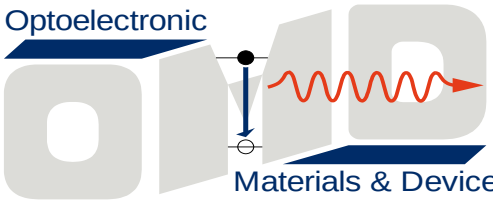

Content

- Motivation
- Basics of X-ray diffraction
- Laue images
- Powder diffractometry
- Pole figures
- Diffractometry
- High resolution X-ray diffraction
- Glazing Incidence

History

2012 was the 100th Aniversery of X-ray Diffraction

- X-rays were discovered by Wilhelm Conrad Röntgen in 1895
- In 1912, Paul Peter Ewald developed a formula to describe the passage of light waves through an ordered array of scattering atoms, based on the hypothesis that crystals were composed of a space-lattice-like construction of particles.
- Maxwell von Laue realized that X-rays might be the correct wavelength to diffract from the proposed space lattice.
- In June 1912, von Laue published the first diffraction pattern in *Proceedings of the Royal Bavarian Academy of Science.*

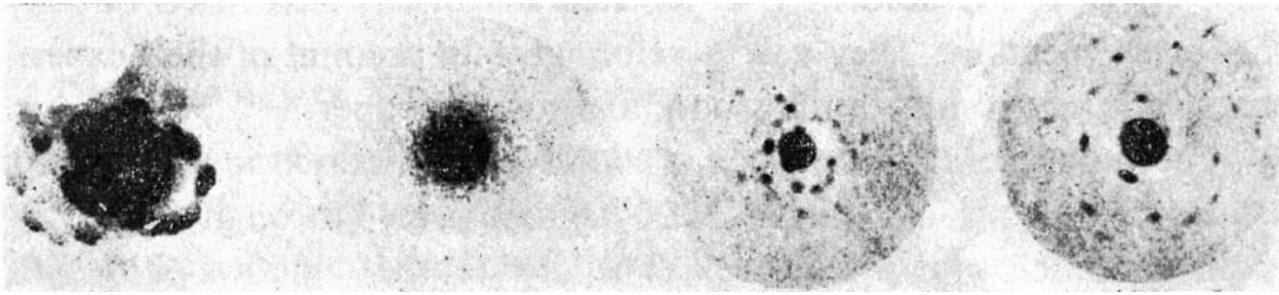

The diffraction pattern of copper sulfate, published in 1912

Basics

Characteristic X-ray radiation

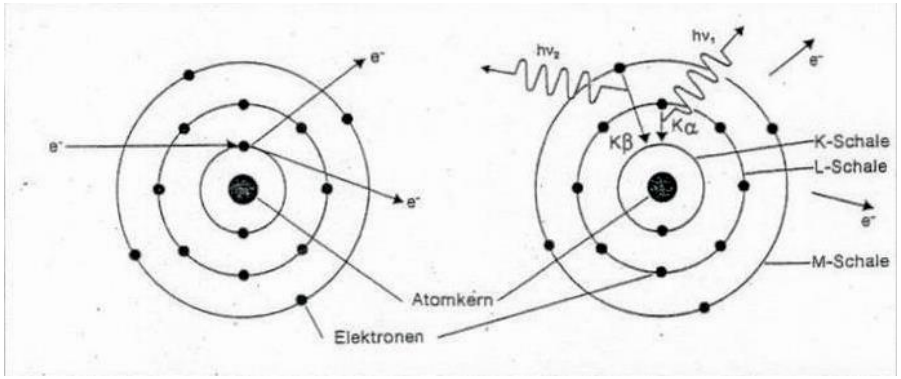

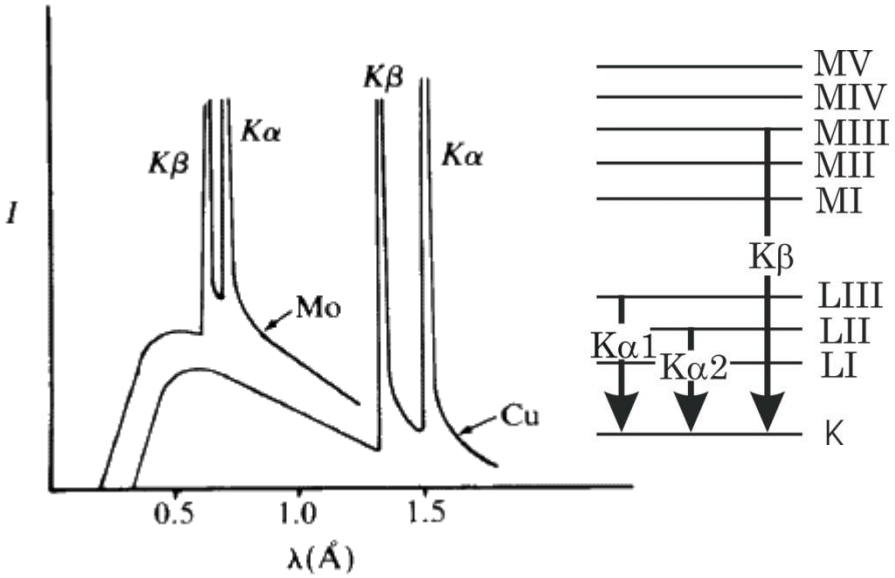

- Electrons from the filament strike the target anode, producing characteristic radiation via the photoelectric effect.
- The electrons knock out electrons of an inner shell (K, L; M etc.), electrons of the outer shells drops down under submission of characteristic X-ray emission.
- Fine structure of the atome shell, orbitals split into sublevels $K_{\alpha 1}$, $K_{\alpha 2}$;..
- The anode material (Cu, Mo, Au, …) determines the wavelengths of characteristic radiation.
- While we would prefer a monochromatic source, the X-ray beam actually consists of several characteristic wavelengths of X rays.

Bragg´s law for diffraction

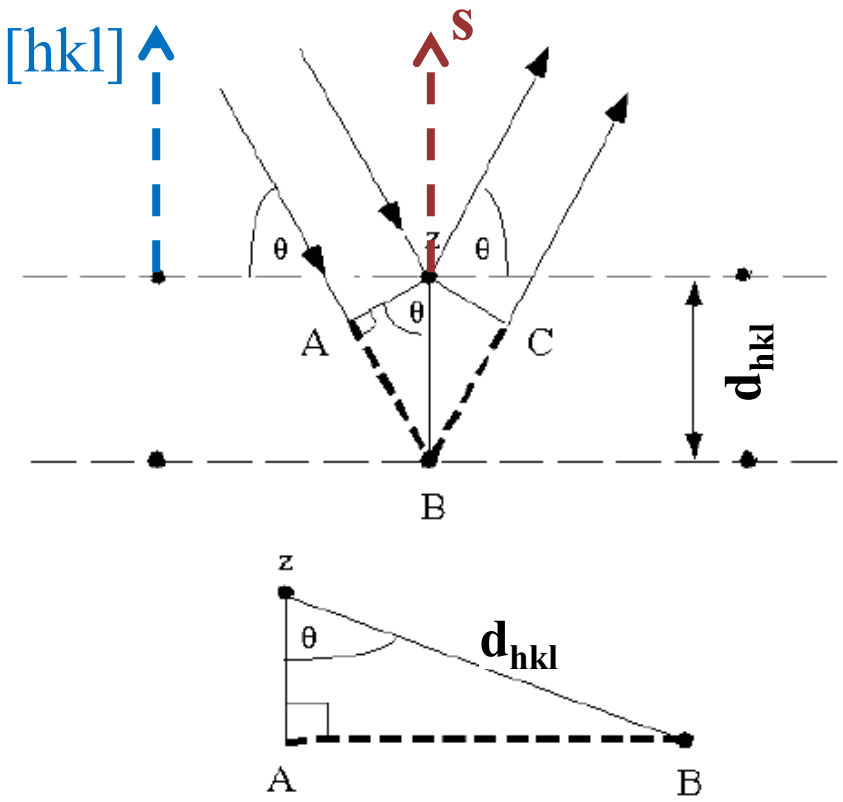

$$n\lambda = 2d_{hkl}\sin\Theta_B$$

- For parallel planes of atoms, with a space d_{hkl} between the planes, constructive interference only occurs when Bragg's law is satisfied.
  - In our diffractometers, the X-ray wavelength λ is fixed.
  - Consequently, a family of planes produces a diffraction peak only at a specific angle θ.
  - **The space between diffracting planes of atoms determines peak positions.**
- Additionally, the plane normal [hkl] must be parallel to the diffraction vector s
  - Plane normal [hkl]: the direction perpendicular to a plane of atoms
  - Diffraction vector s: the vector that bisects the angle between the incident and diffracted beam

Structure factor

The diffraction peak intensity is determined by the arrangement of atoms in the entire crystal

$$I_{hkl} \propto |F_{hkl}|^2$$

$$F_{hkl} = \sum_{j=1}^{m} N_j f_j \exp\left[2\pi i\left(hx_j + ky_j + lz_j\right)\right]$$

- The structure factor F_{hkl} sums the result of scattering from all of the atoms in the unit cell to form a diffraction peak from the (hkl) planes of atoms
- The amplitude of scattered light is determined by:
  - where the atoms are on the atomic planes
    - this is expressed by the fractional coordinates x_j y_j z_j
  - what atoms are on the atomic planes
    - the scattering factor f_j quantifies the efficiency of X-ray scattering at any angle by the group of electrons in each atom
      - The scattering factor is equal to the number of electrons around the atom at 0° θ, the drops off as θ increases
    - N_j is the fraction of every equivalent position that is occupied by atom j

X-ray beam path and goniometer motions

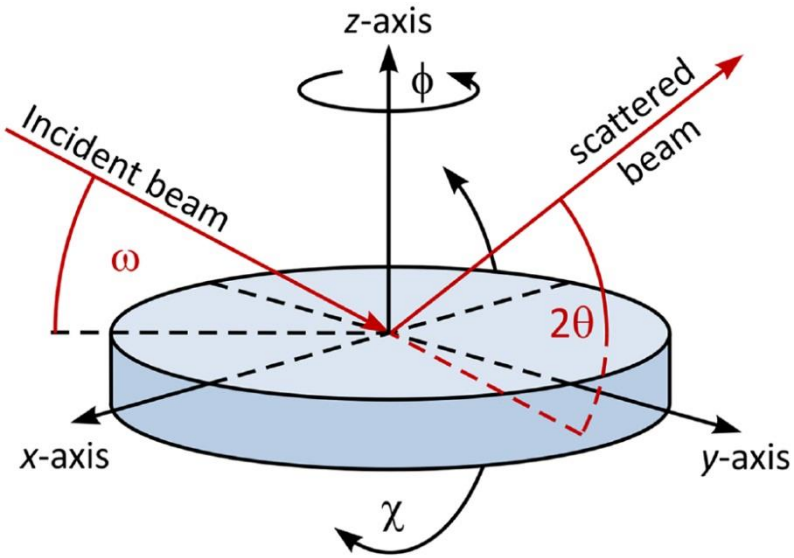

Figure 2. Illustration of the beam path and the different goniometer motions.

M. Frentrup et al., J. Phys. D: Appl. Phys. **50** (2017) 433002

X-ray equipment

Generation of X-rays

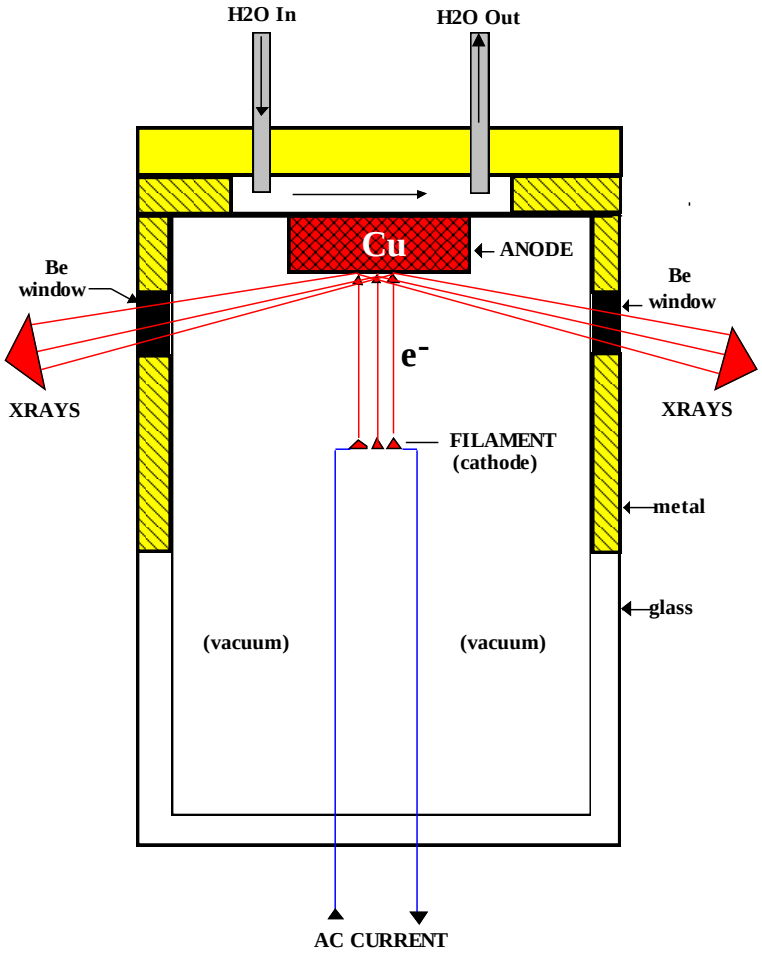

- Sealed X-ray tubes tend to operate at 1.8 to 3 kW.
- Rotating anode X-ray tubes produce much more flux because they operate at 9 to 18 kW.
  - A rotating anode spins the anode at 6000 rpm, helping to distribute heat over a larger area and therefore allowing the tube to be run at higher power without melting the target.
- **Both sources generate X rays by striking the anode target with an electron beam from a tungsten filament.**
  - The target must be water cooled.
  - The target and filament must be contained in a vacuum.
- Exit window: Be

PANalytical X´Pert Pro MPD

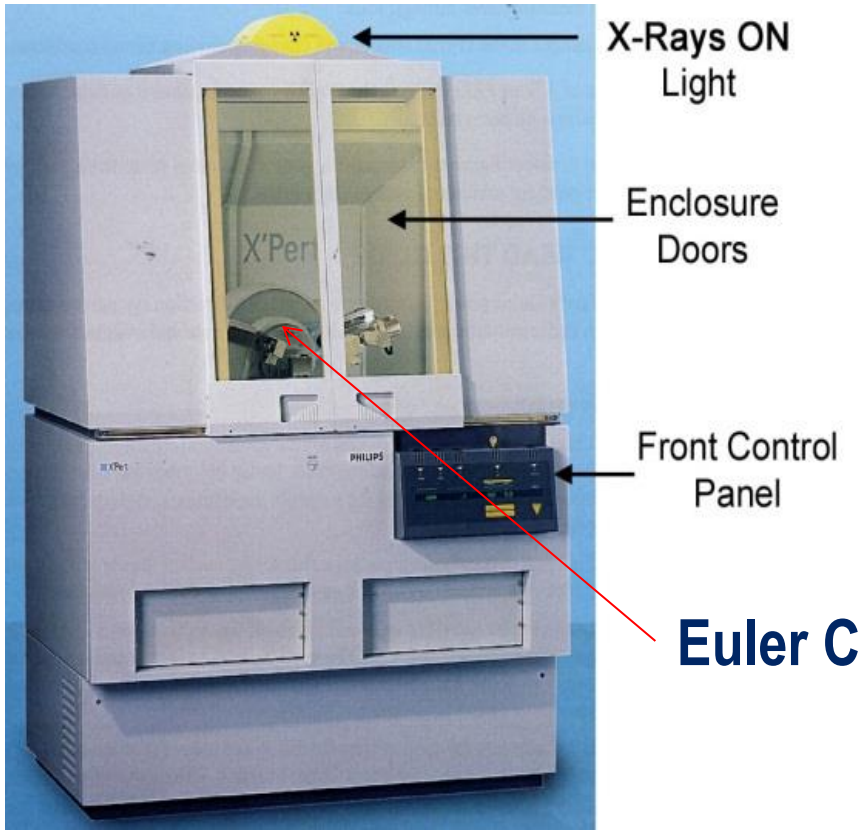

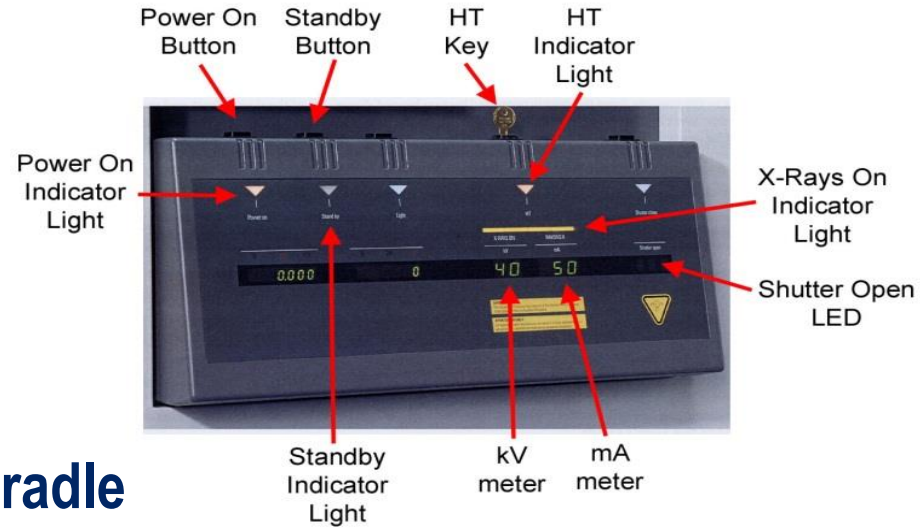

PANalytical X´Pert Pro MPD

Tube and programable slit

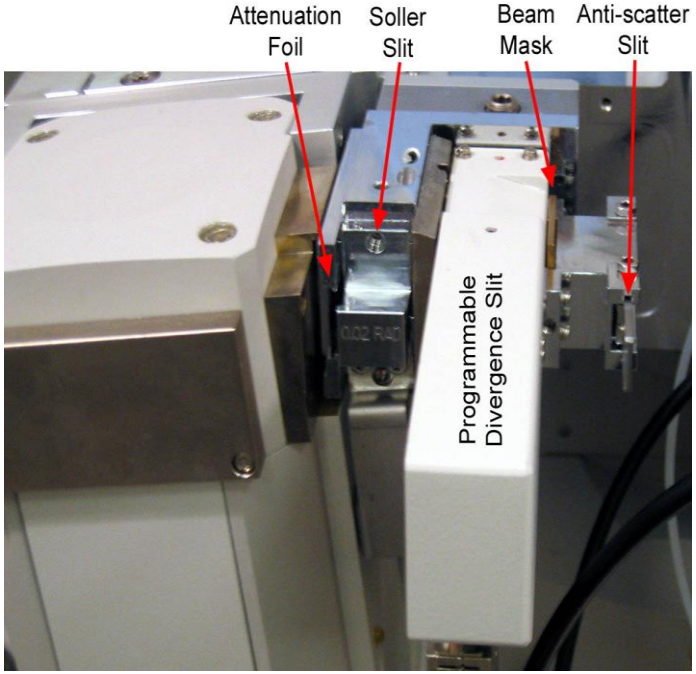

Detection side

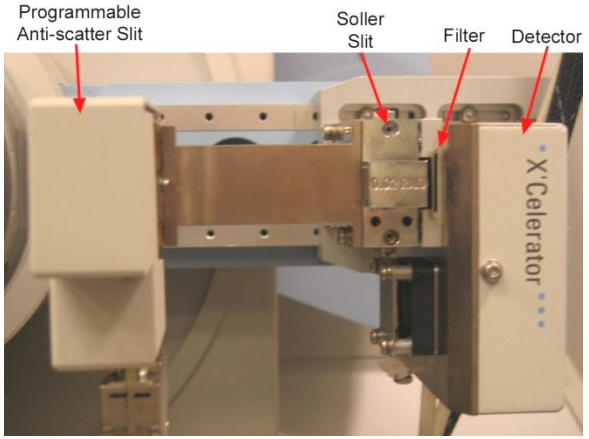

Filter

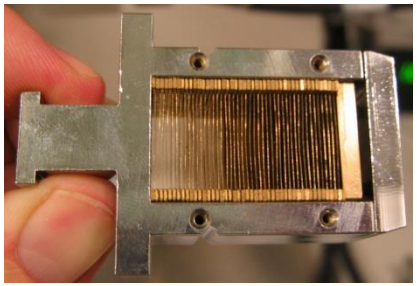

This image shows a 4-bounce Ge monochromator

- Each pair of diffracting crystals is channel-cut from a single piece of Ge
  - This prevents misorientation between the pair of crystals
- Two sets of channel-cut crystals are used
  - The orientation between these two sets must be precisely aligned to get a usable X-ray beam
- Slits are used to control the width of the beam entering the first channel-cut crystal and to control the width in-between the two sets of channel-cut crystals

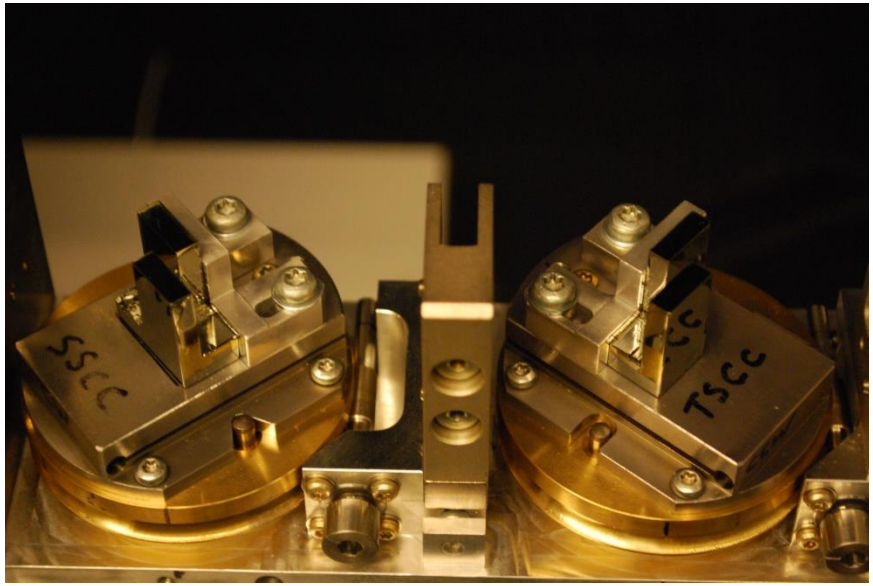

Euler Cradle

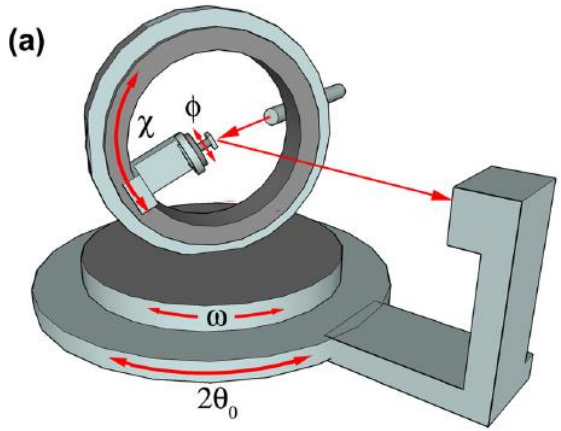

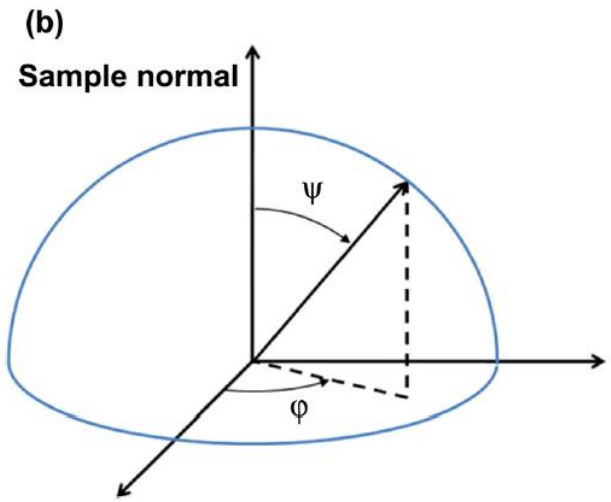

Schematic drawing of a diffractometer

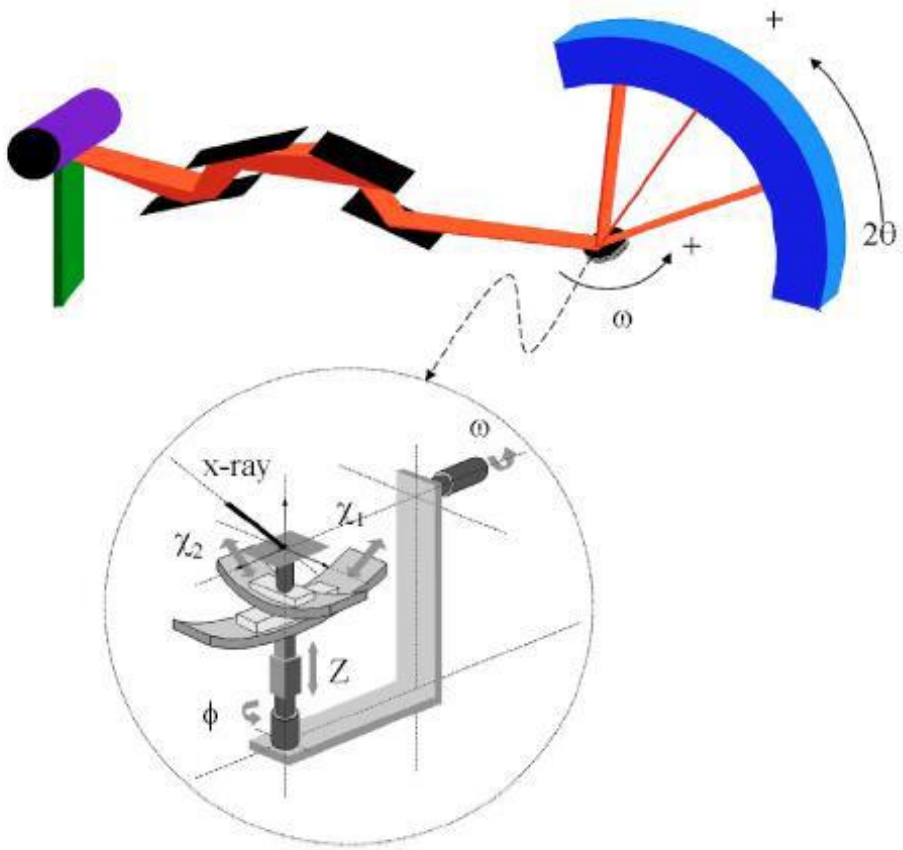

FIG. 1. (Color online): Schematic drawing of the diffractometer and the five-movement sample holder.

O. Masson et al., Rev. Sci. Instrum. **76**, 063912 (2005)

Laue measurements

Laue diffraction

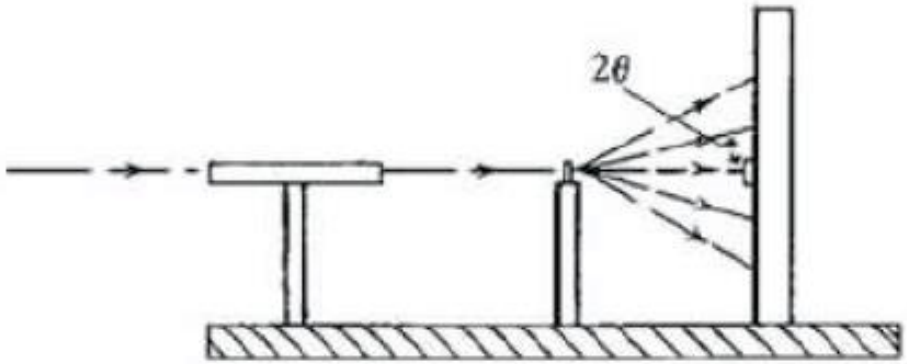

A stationary mounted crystal will be irradiated by a white X-ray beam. Since Θ and d are specified by the crystal orientation, one gets a stereografical projection of the (reciprocal) lattice plans at angles 2Θ as points with equal nλ/d.

$$n\lambda = 2d_{hkl}\sin\Theta_B$$

Bragg condition

The images are taken in transmission (forward scattering) for small crystals or in reflection (backward scattering) on X-ray films, luminescence folie, or X-ray image sensors.

Since the crystal structure (d) is mostly known, Laue images are mainly used to determine the orientation (Θ) of the single crystal (e.g. substrate).

Laue diffraction pattern

- Von Laue's diffraction pattern supported two important hypotheses
  - X-rays were wavelike in nature and therefore were electromagnetic radiation
  - The space lattice of crystals
- Bragg consequently used X-ray diffraction to solve the first crystal structure, which was the structure of NaCl published in June 1913.
- Single crystals produce "spot" patterns similar to that shown to the right.
- *However, powder diffraction patterns look quite different.*

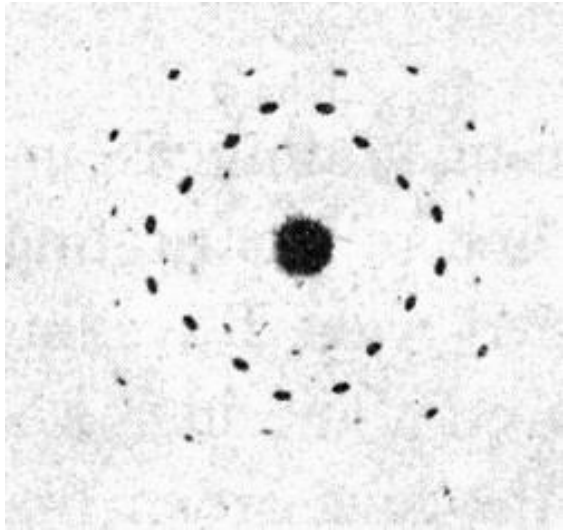

The second diffraction pattern published was of ZnS. Because this is a higher symmetry material, the pattern was less complicated and easier to analyze

Laue image of wurtzit ALN in c-direction

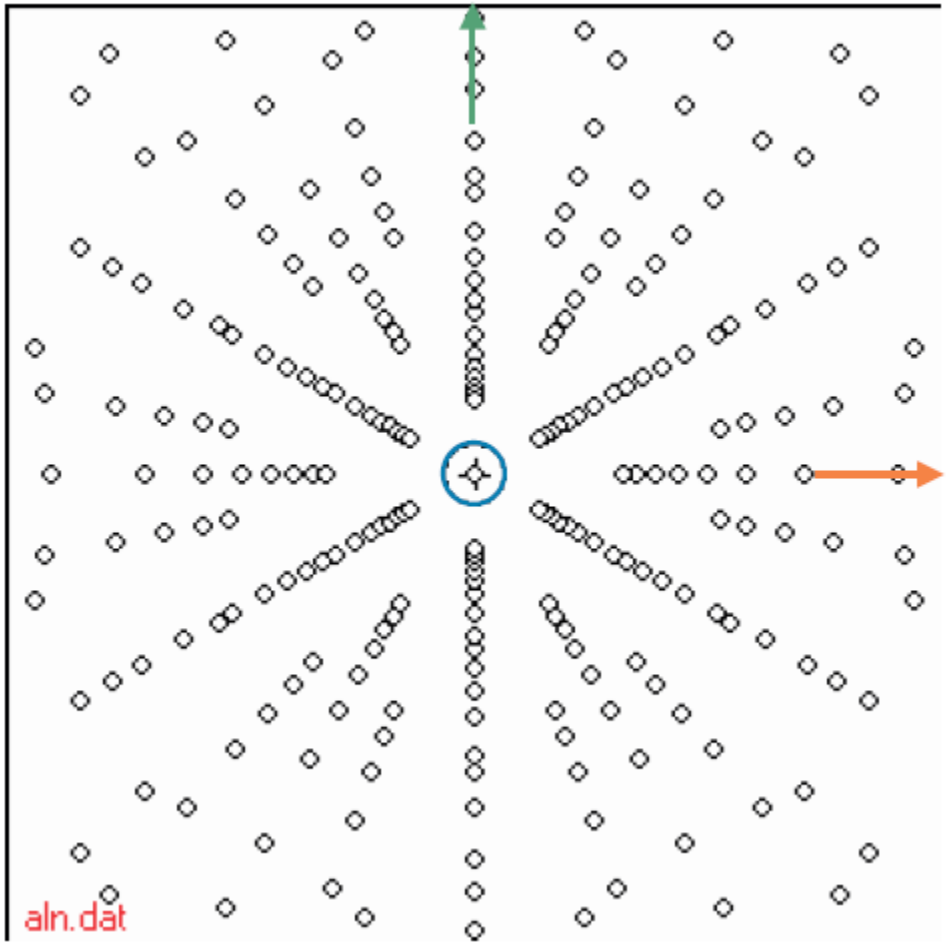

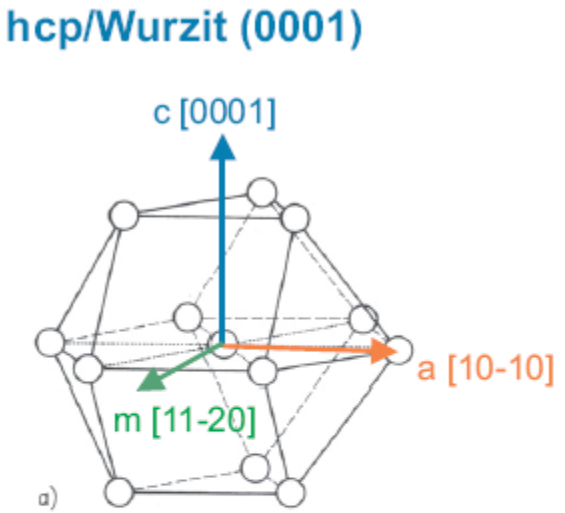

Typically angle sections of $-30° < \Theta < 30°$ are recorded in respect to the incident beam.

Laue image of wurtzit ALN in m-, a-direction and 14° off-oriented

hcp/Wurzit m (10-10)

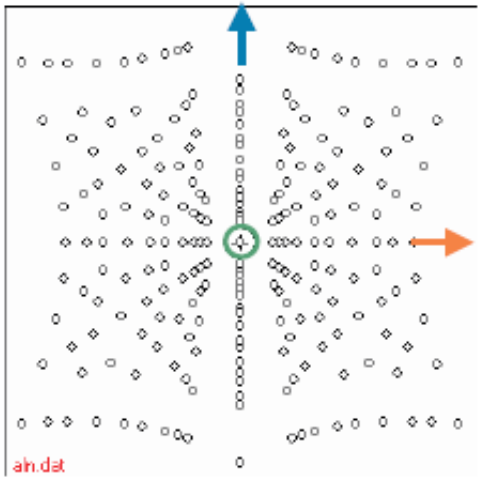

hcp/Wurzit a (11-20)

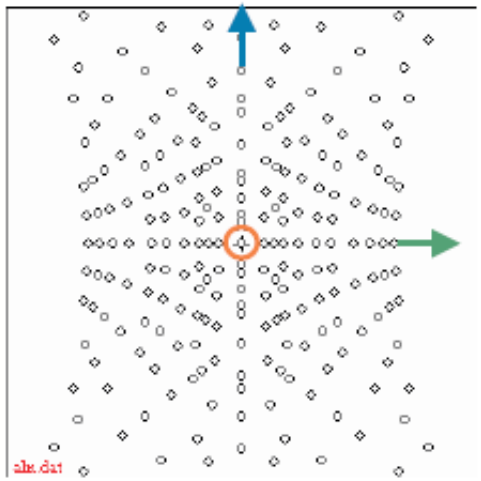

hcp/Wurzit off-orientiert

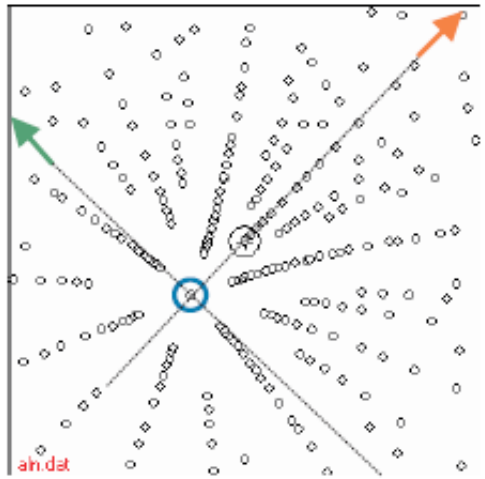

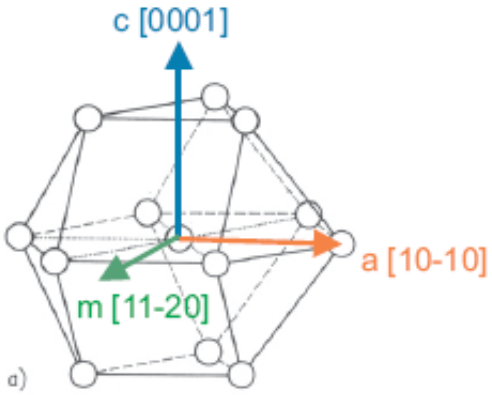

14° off orientied in relation to the c-axes in the direction to the a-axes (and crystal is rotated by 45°)

Determination of the off-orientation x to the plane

$$x = 1/2 \arctan(L/D)$$

L = distance on the film
D = distance film – crystal

Laue images of cubic zincblende structure

fcc/Zinkblende (100)

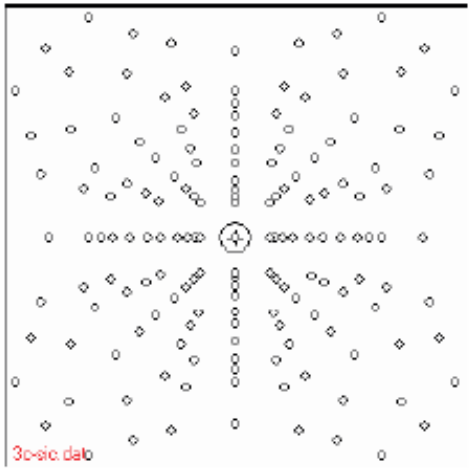

4-fold

fcc/Zinkblende (110)

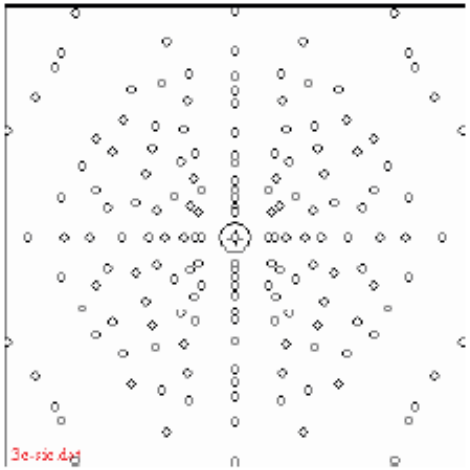

mirror

fcc/Zinkblende (111)

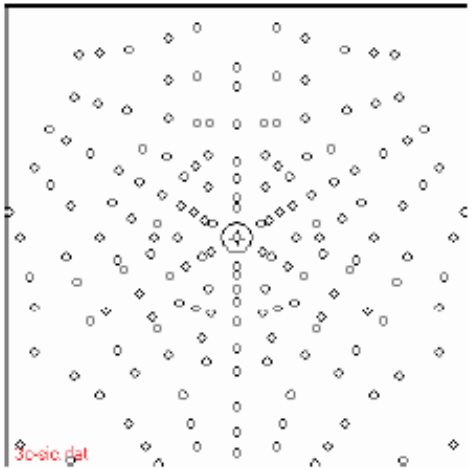

3-fold

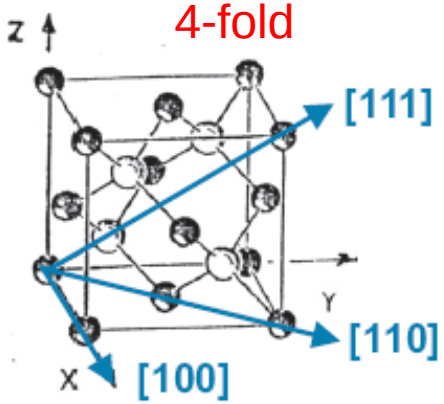

space group F $\bar{4}$3m

{100} {111} {110}

Powder diffraction

Powder diffraction

An X-ray powder diffraction pattern is a plot of the intensity of X-rays scattered at different angles by a sample

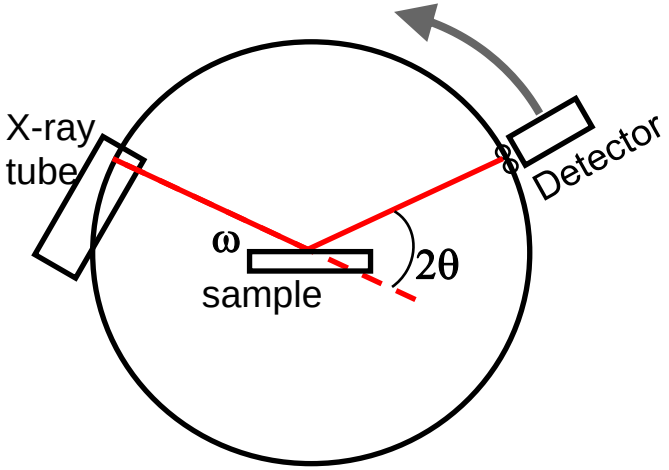

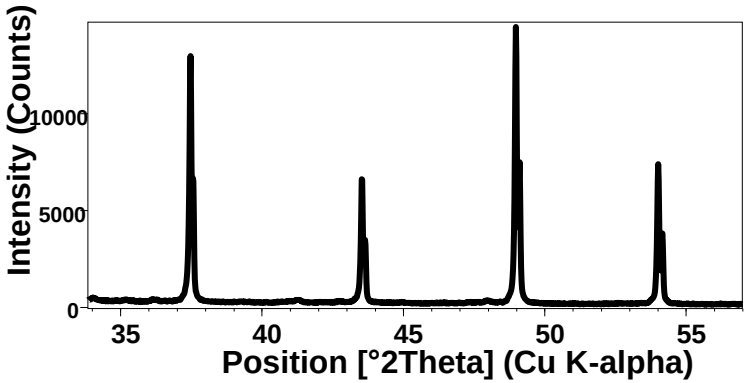

- The detector moves in a circle around the sample
  - The detector position is recorded as the angle 2theta (ω-2θ)
  - The detector records the number of X-rays observed at each angle 2θ
  - The X-ray intensity is usually recorded as “counts” or as “counts per second”
- Many powder diffractometers use the Bragg-Brentano parafocusing geometry
  - To keep the X-ray beam properly focused, the incident angle omega changes in conjunction with 2theta
  - This can be accomplished by rotating the sample or by rotating the X-ray tube.

Powder diffraction

In an ideal powder all crystal orientations are equally distributed

- Comparision with standard measurements („PDF-Files“)

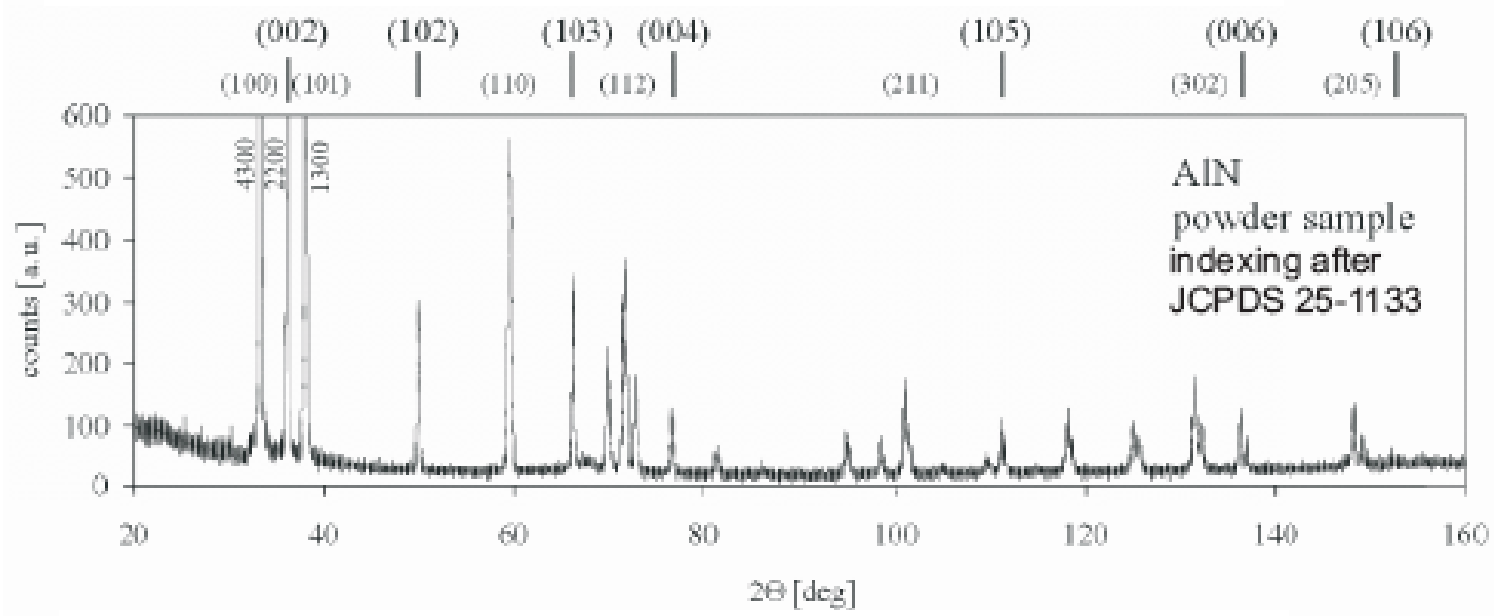

- Identification of foreign phases
  (diffraction at angles Θ different to that the main crystal)

Diffractometry of thin layers

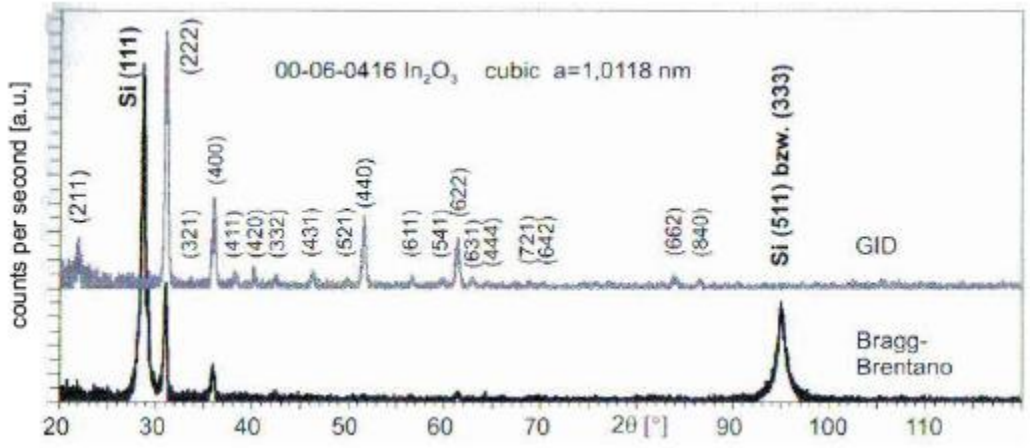

– Messung dünner Schichten mit streifendem Einfall (Grazing Incidence XRD)
⇒ Die Röntgenstrahlen treffen nur Netzebenen in der Oberflächenschicht

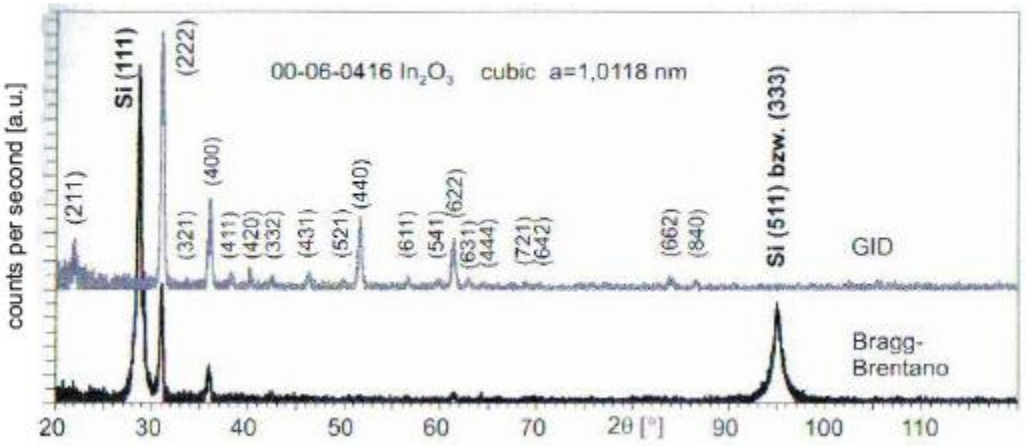

Beispiel: In_2O_3 auf Si(111)-Substrat

Pole figures

Texture mapping

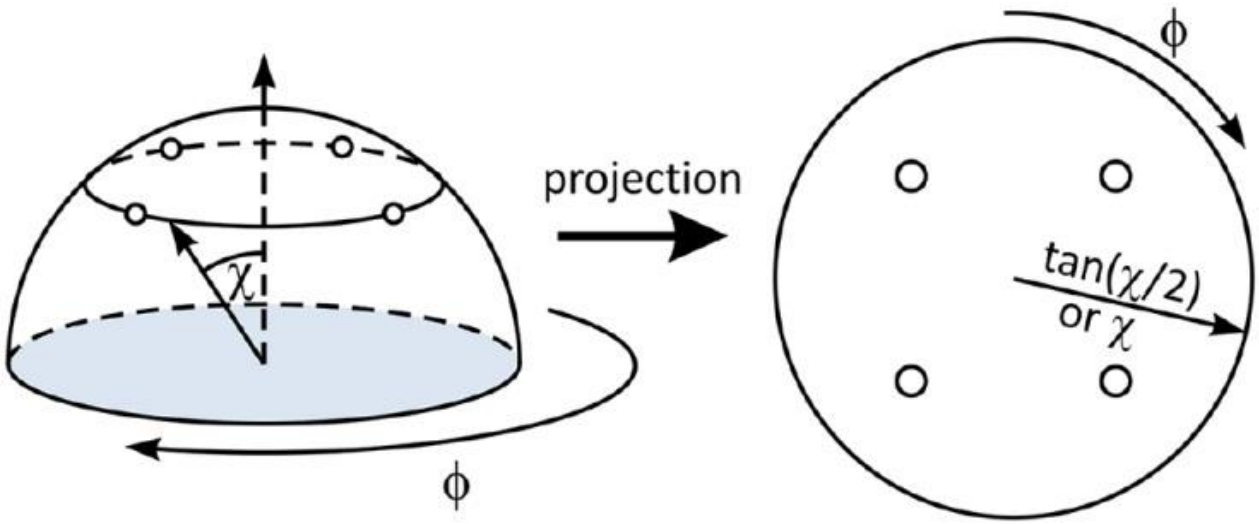

Diagram explaining the measurement geometry to map a texture in reciprocal space and its projection onto a 2D map.

Ni single crystal pole figure

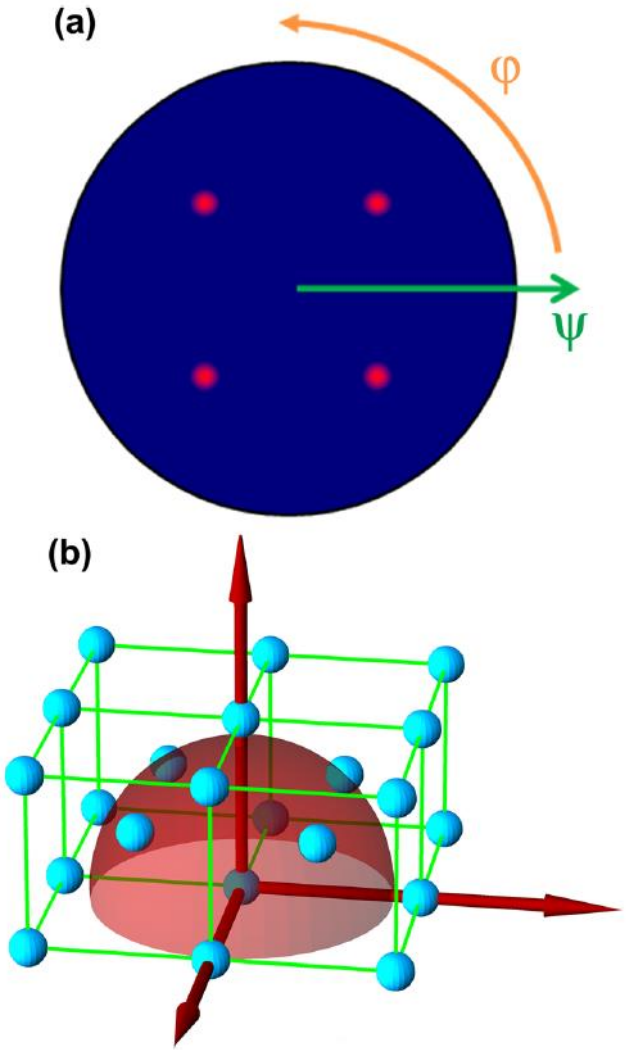

(a) Schematic representation of a Ni single crystal pole figure at d = 2.03 Å.

(b) Reciprocal space representation of the Ni reciprocal lattice and pole figure (red half sphere) in three dimensions.

Preferred Orientation (texture)

- Preferred orientation of crystallites can create a systematic variation in diffraction peak intensities
  - can qualitatively analyze using a 1D diffraction pattern by looking at how observed peak intensities deviate systematically from the ideal
  - a pole figure maps the intensity of a single peak as a function of tilt and rotation of the sample
    - this can be used to quantify the texture

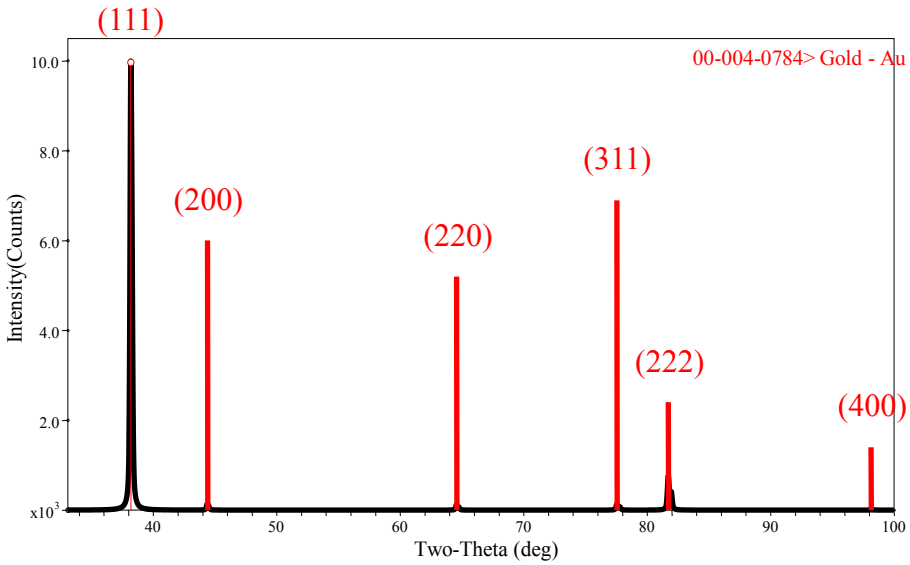

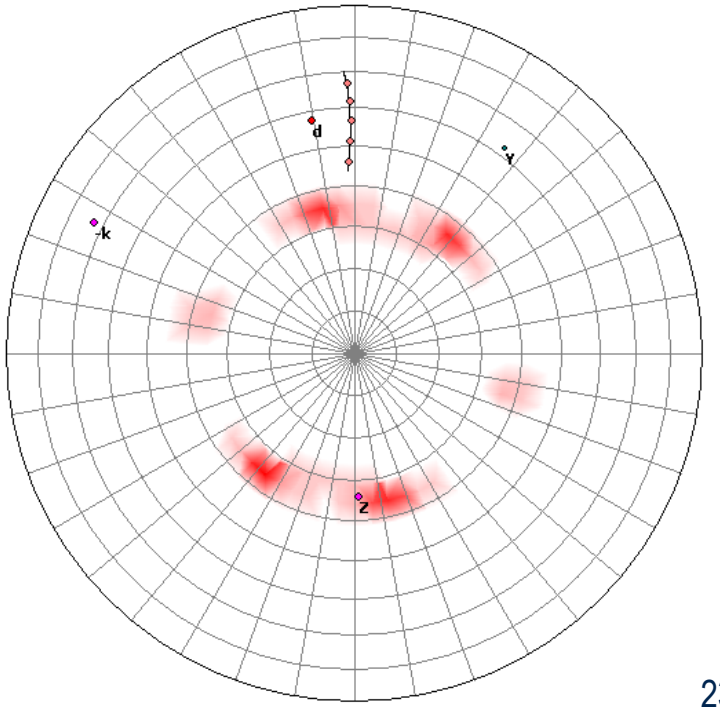

Pole figures of cubic GaN on 3C-SiC

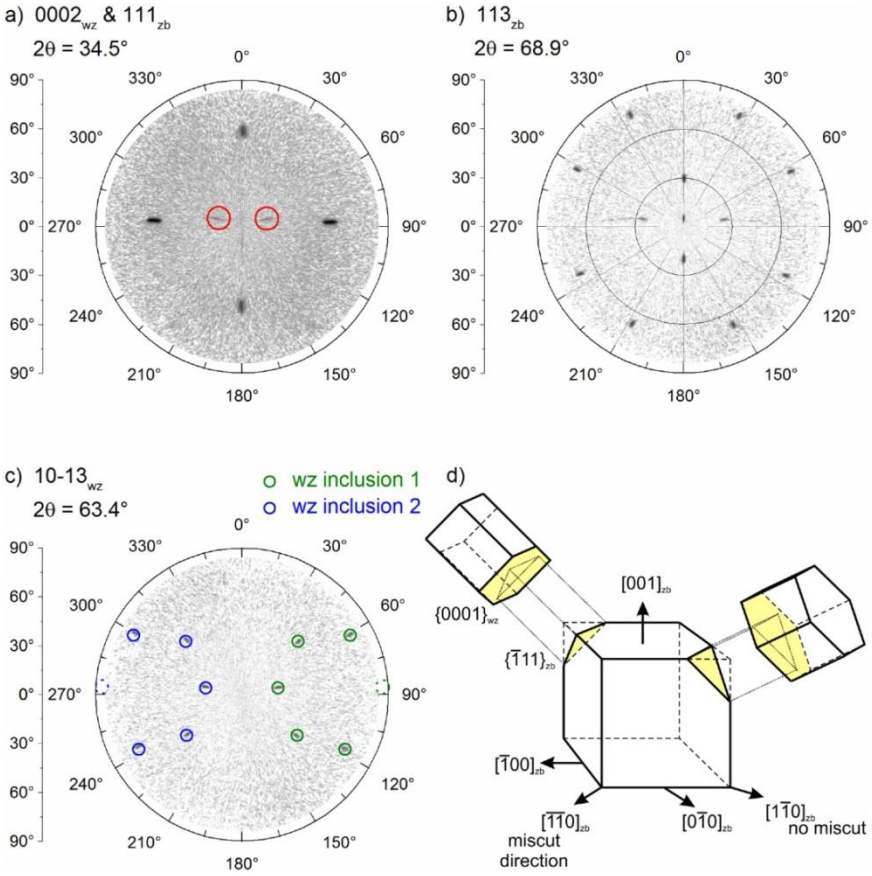

Pole figures for different wurtzite and zincblende reflections of GaN grown on (0 0 1) *zb* oriented 3C-SiC/Si-templates (a)–(c). The diagram illustrates the crystallographic arrangement of both phases.

High resolution XRD

Motivation

HRXRD and XRR are both used to study thin films and benefit from the same optics, so we often consider them together

HRXRD can measure:

- Structural Information
  - Composition
  - Thickness
  - Superlattice period
- Defects
  - Mismatch
  - Relaxation
  - Misorientation
  - Dislocation Density
  - Mosaic Spread
  - Curvature
  - Inhomogeneity
  - Surface Damage

XRR can measure:

- Thickness
- Surface and Interface Roughness
- Density or composition of the topmost layer

Various scan types

Table 2. Scan types available on high-resolution diffractometers. ω refers to the angle between the incident beam and the sample surface, 2θ refers to the angle between the incident and diffracted beams.

Scan type	Description
2θ–ω	The sample (or the x-ray source) is rotated by ω and the detector is rotated by 2θ with an angular ratio of 1 : 2. In reciprocal space, $\boldsymbol{S}$ moves outwards from the origin. The *length* of $\boldsymbol{S}$ changes, but its *direction* remains the same and depends on the offset. For 2θ–ω scans, the x-axis is in units of 2θ, whereas for ω–2θ scans, the x-axis is in units of ω. When there is no offset and $\omega = \theta$ this is a symmetrical scan (θ–2θ) which is vertical in reciprocal space. Standard scan type for powder diffraction.
ω–2θ	Simply a 2θ–ω scan, but with ω on the x-axis. Standard scan type for reflectivity and high-resolution work.
2θ	The sample and source remain stationary and the detector is moved. $\boldsymbol{S}$ traces an arc along the circumference of the Ewald sphere. Both the *length* and the *direction* of $\boldsymbol{S}$ change.
ω-scan	The detector remains stationary and the sample is rotated about the ω axis. In reciprocal space, $\boldsymbol{S}$ traces an arc centred on the origin. The *length* of $\boldsymbol{S}$ stays the same, but its *direction* changes.
Q-scan	Software can be used to scan ω and 2θ in non-integer ratios, scanning $\boldsymbol{S}$ along a given direction in reciprocal space. Reciprocal space maps of any desired shape (in reciprocal space) can then be collected[a].
ϕ	Rotation of the sample about the ϕ axis (usually in the plane of the sample). The *length* of $\boldsymbol{S}$ stays the same, but the sample is moved, bringing the reciprocal lattice spot through $\boldsymbol{S}$ so that the *direction* of $\boldsymbol{S}$ changes with respect to the sample.
χ	Similar to ϕ scans, except that the sample is rotated about the χ axis (plane of the sample rotated with respect to the incoming beam).

M A Moram and M E Vickers Rep. Prog. Phys. **72** (2009) 036502

Diffractometer

Schematic plot of the of the Philips X´pert material research diffractometer consisting of the X-ray tube, hybrid monochromator, euler cradle and detector.

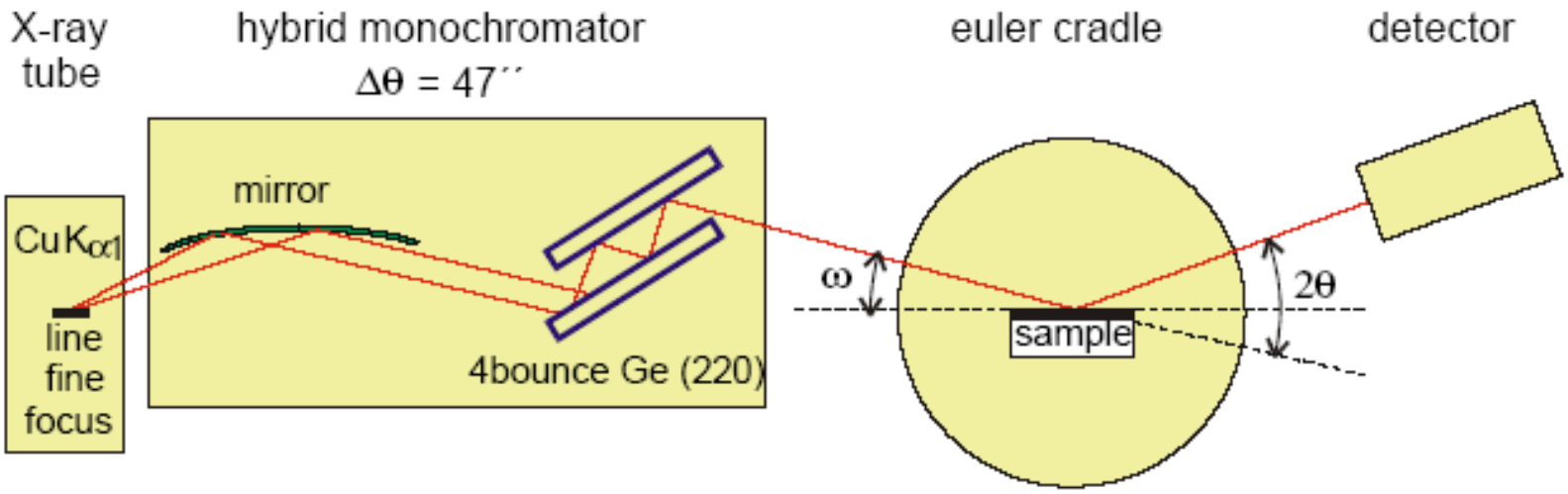

Reciprocal space

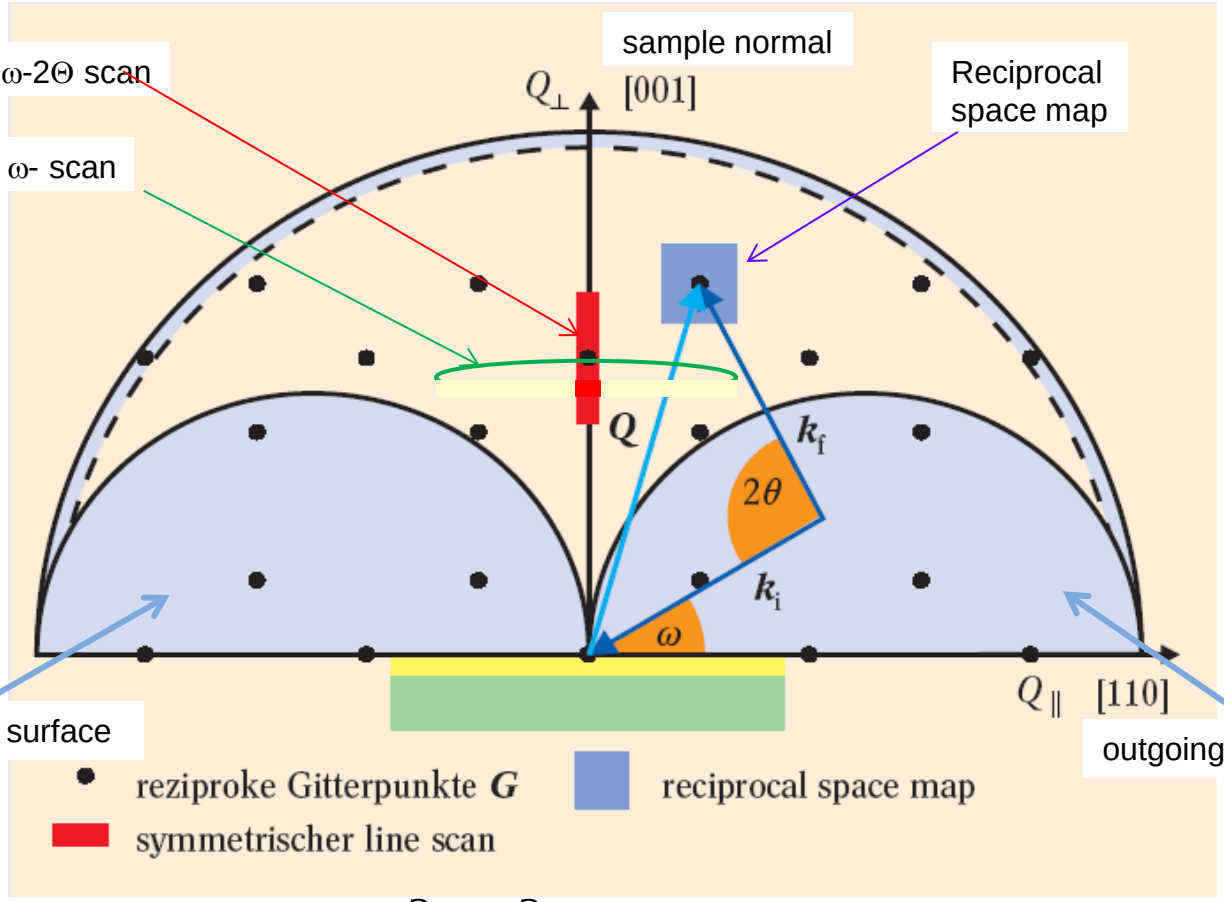

$$Q_\perp = Q_z = \frac{2\pi}{a_\perp} = \frac{2\pi}{\lambda}\left[\cos(\theta-\omega)-\cos(\theta+\omega)\right]$$

$$Q_\square = Q_x = \frac{2\pi}{a_\square} = \frac{2\pi}{\lambda}\left[\sin(\theta-\omega)+\sin(\theta+\omega)\right]$$

Scattering vectors Q

$$Q = K - K_0$$

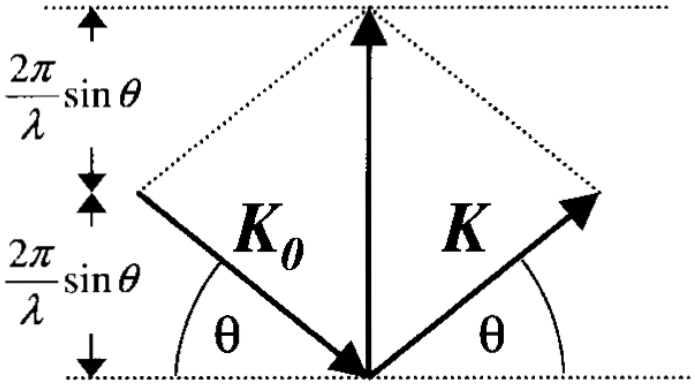

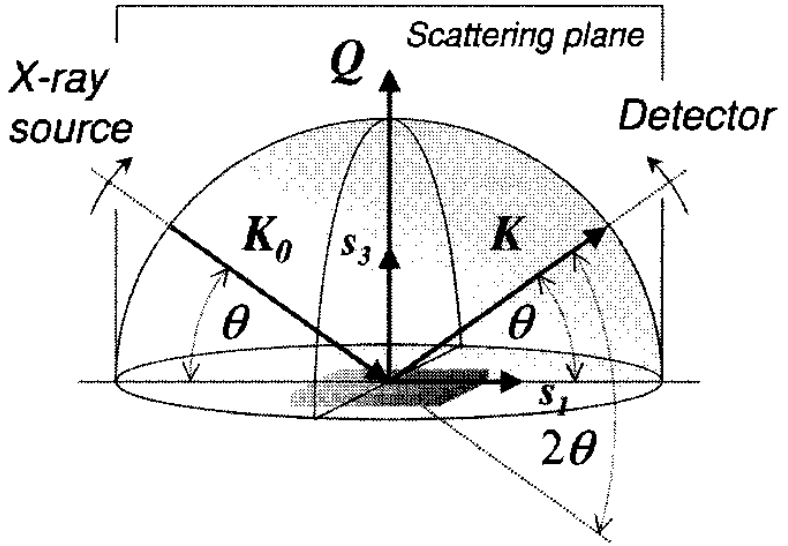

Scattering vector Q:

$$Q_{\perp} = Q_z = \frac{2\pi}{a_{\perp}} = \frac{2\pi}{\lambda}\left[\cos(\theta-\omega) - \cos(\theta+\omega)\right]$$

$$Q_{\parallel} = Q_x = \frac{2\pi}{a_{\parallel}} = \frac{2\pi}{\lambda}\left[\sin(\theta-\omega) + \sin(\theta+\omega)\right]$$

$$\frac{1}{d} = \sqrt{Q_x^2 + Q_z^2} = \sqrt{Q_{\parallel}^2 + Q_{\perp}^2}$$

ω-2Θ scans

SiGe on Si

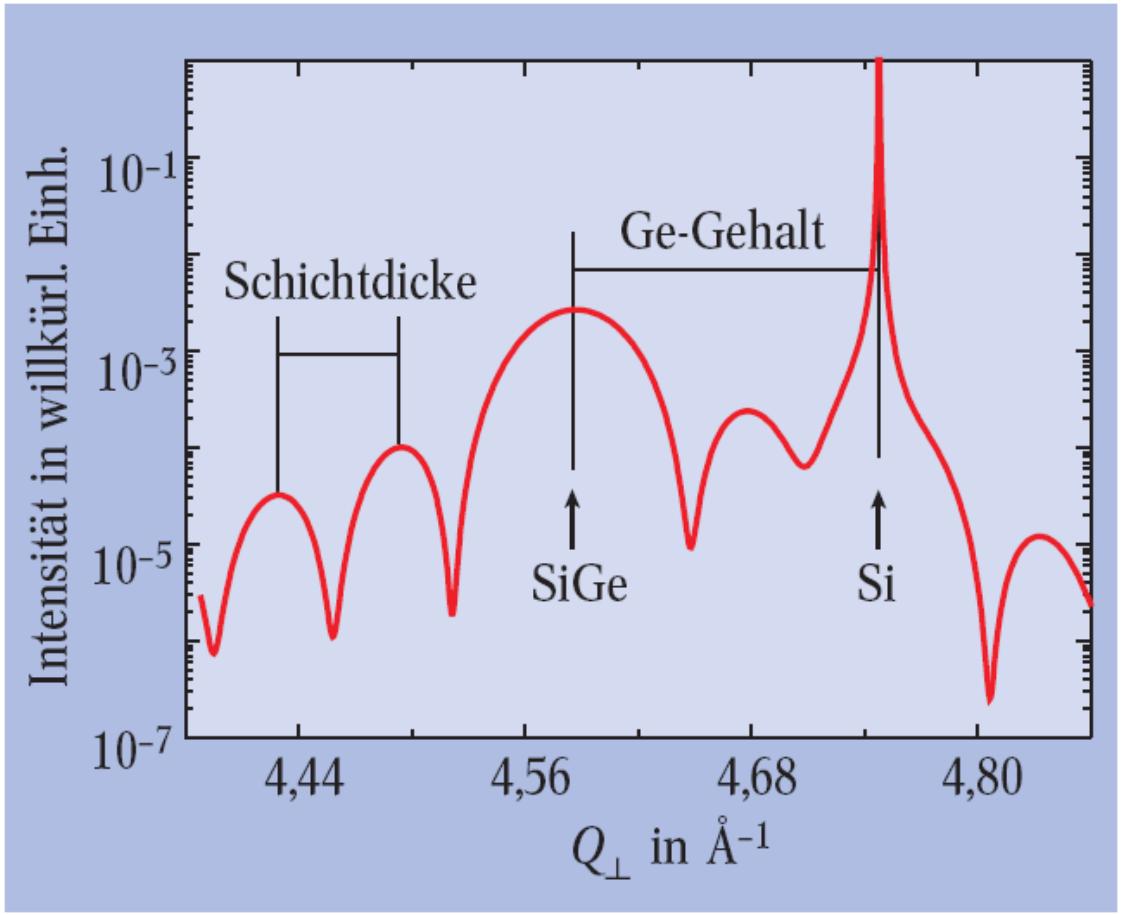

A typical diffraction spectrum of a symmetric „single scans“ of an SiGe-epilayer on Si.

HRXRD of Si/SiGe superlattice deposited on (001) Si

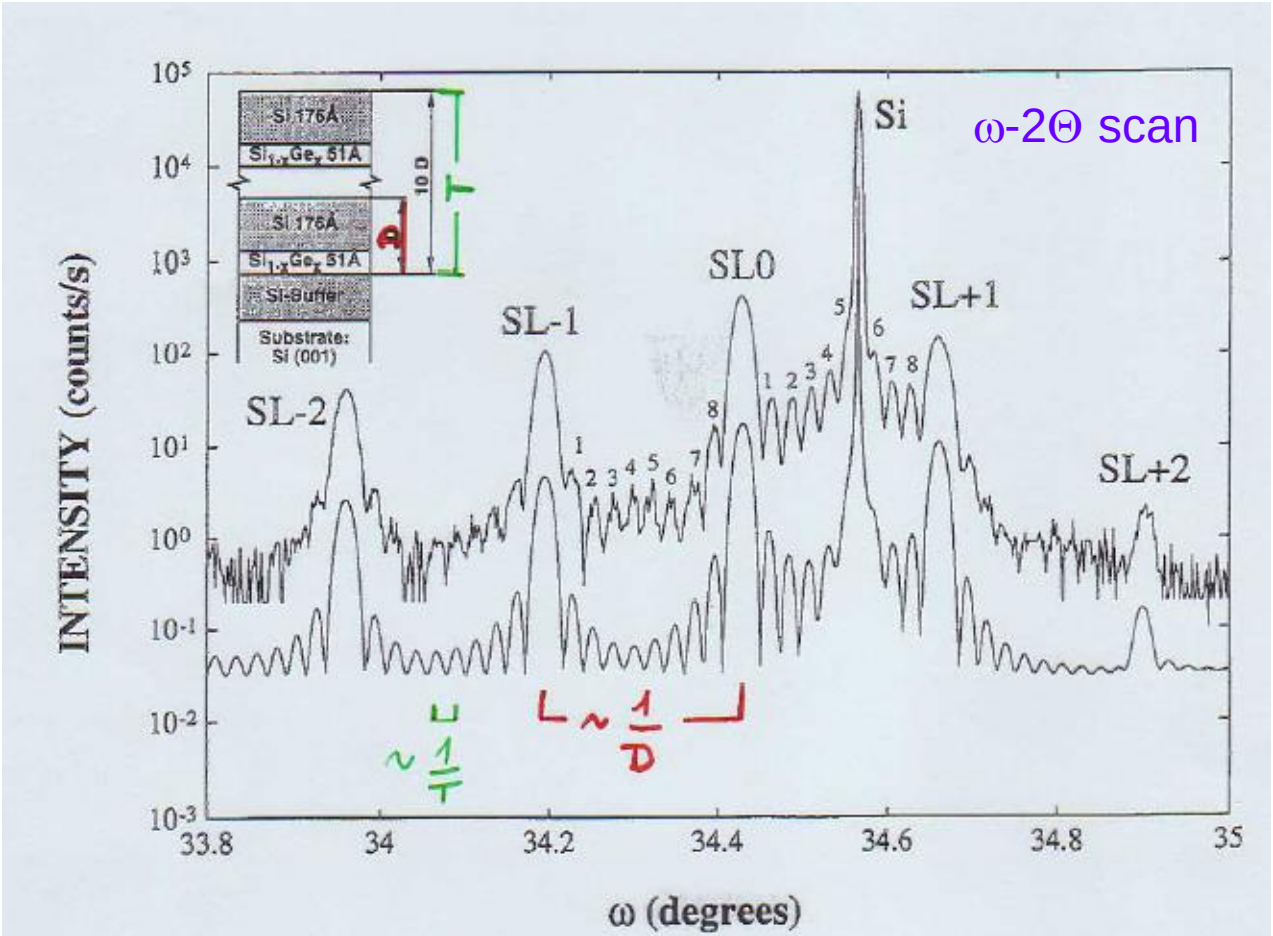

Fig. 6.44. HRXRD of Si/SiGe superlattice deposited on (001) oriented Si. SL period $D = 227$ Å with 10 double layers corresponding to a total thickness of 2270 Å. The number of secondary maxima in-between the main SL satellite peaks is $10 - 2 = 8$

(002) ω–2θ scan from MQWs

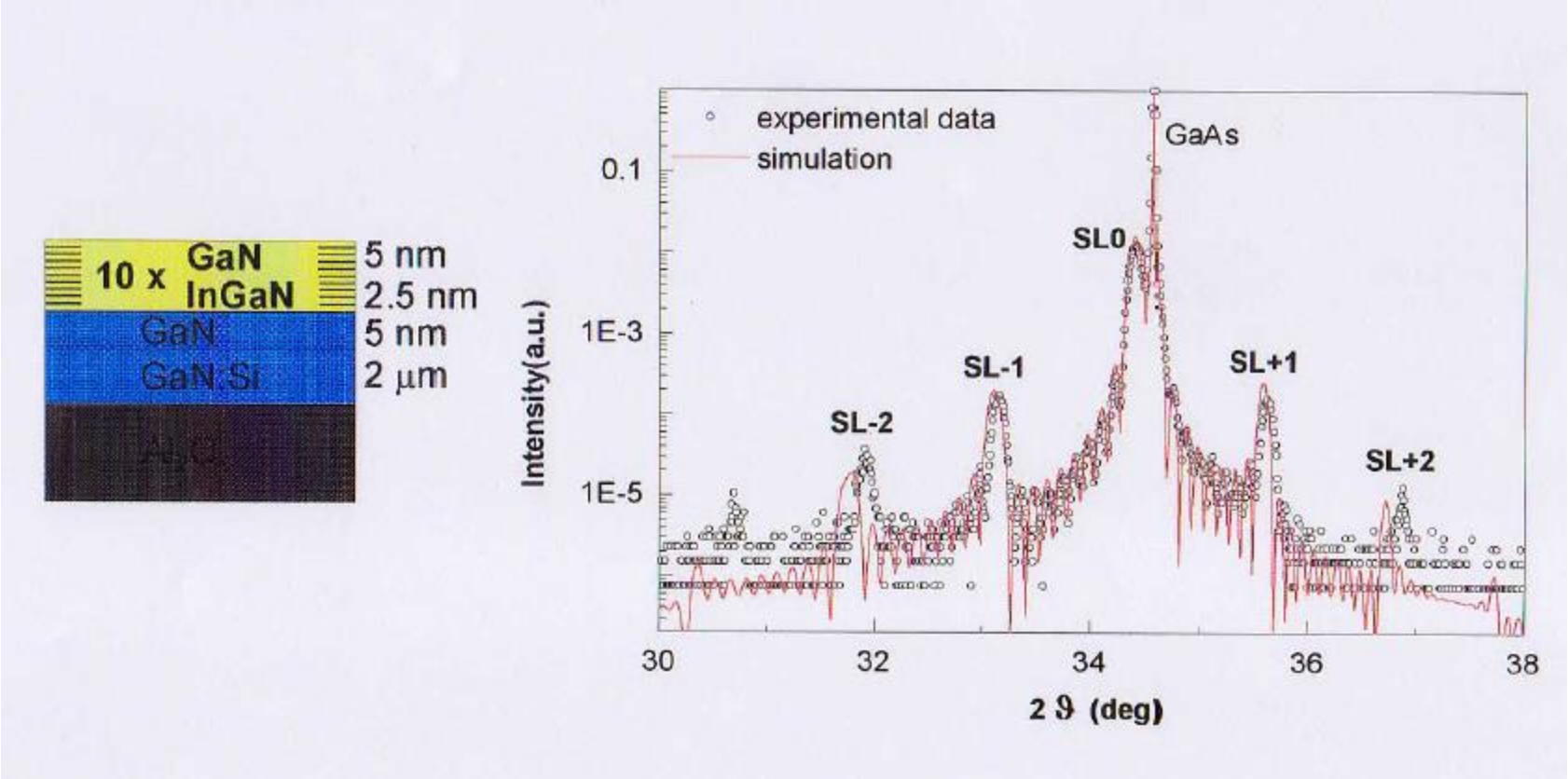

Rocking curve
(ω-scan)

Rocking curve

A rocking curve (ω-scan) produces observed intensity from planes that are not perfectly parallel

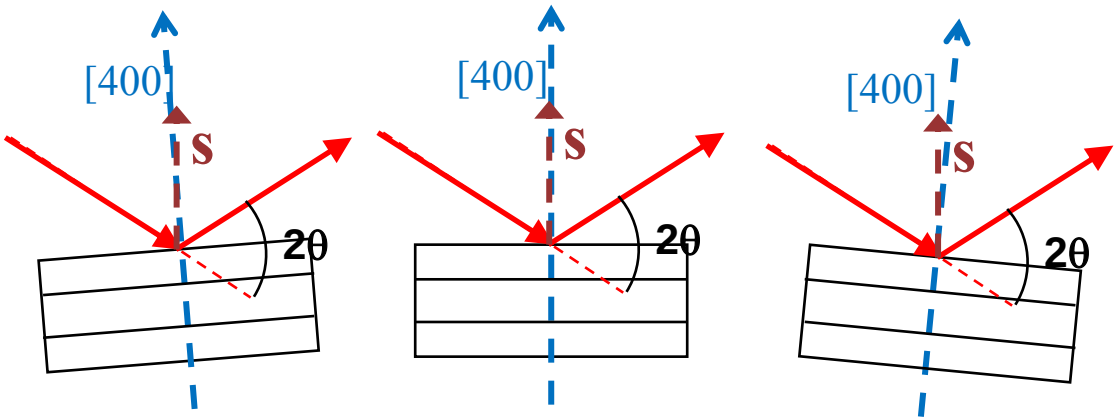

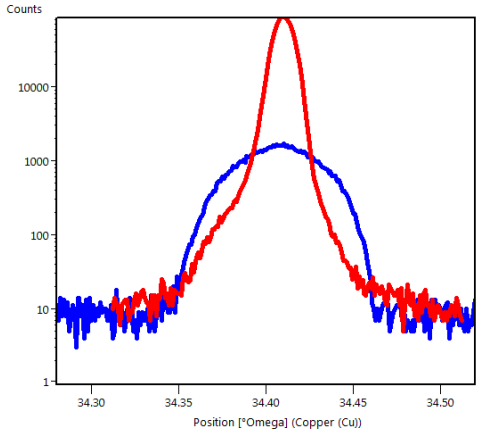

- In a rocking curve, the detector is set at a specific Bragg angle and the sample is tilted.
- A perfect crystal will produce a very sharp peak, observed only when the crystal is properly tilted so that the crystallographic direction is parallel to the diffraction vector s
  - The RC from a perfect crystal will have some width due to instrument broadening and the intrensic width of the crystal material
- Defects like mosaicity, dislocations, and curvature create disruptions in the perfect parallelism of atomic planes
  - This is observed as broadening of the rocking curve
  - The center of the rocking curve is determined by the d-spacing of the peaks

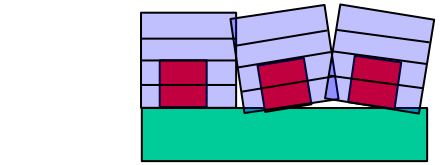

Linewidth dependence of cubic GaN epilayers vs film thickness

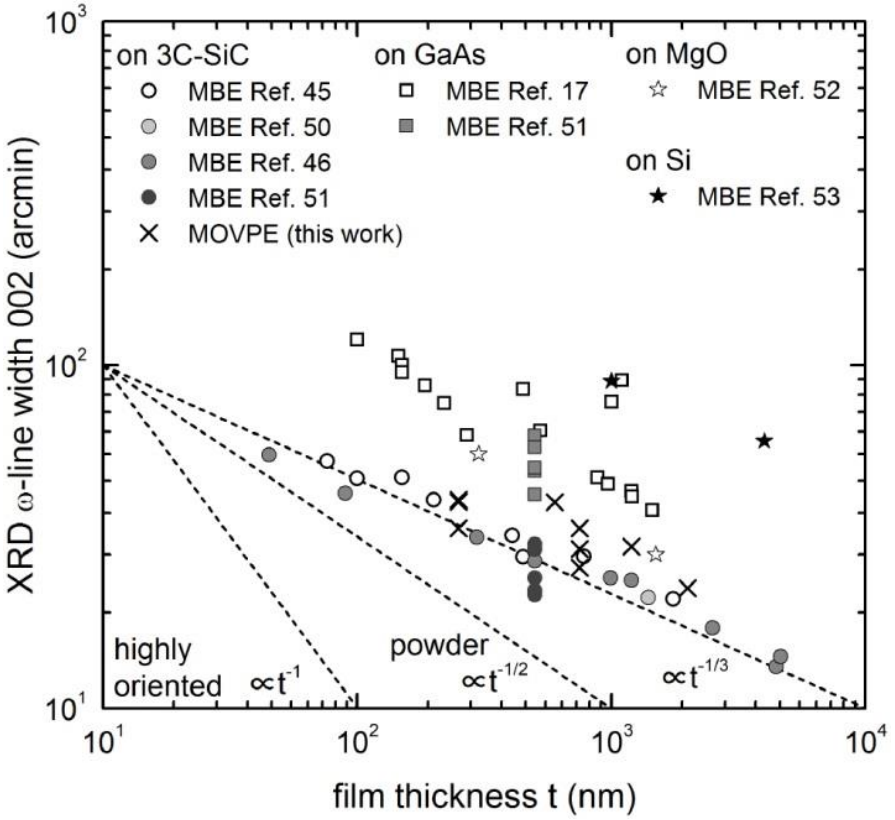

Decrease of the XRD ω-linewidth (FWHM) with increasing film thickness for oriented zincblende GaN grown on relevant substrates 3C-SiC, GaAs, MgO, and Si.

→ Reduction in the defect density and an improvement in the material quality for thicker epitaxial films

M. Frentrup et al., J. Phys. D: Appl. Phys. **50** (2017) 433002

Bowing of 3C-SiC wafer

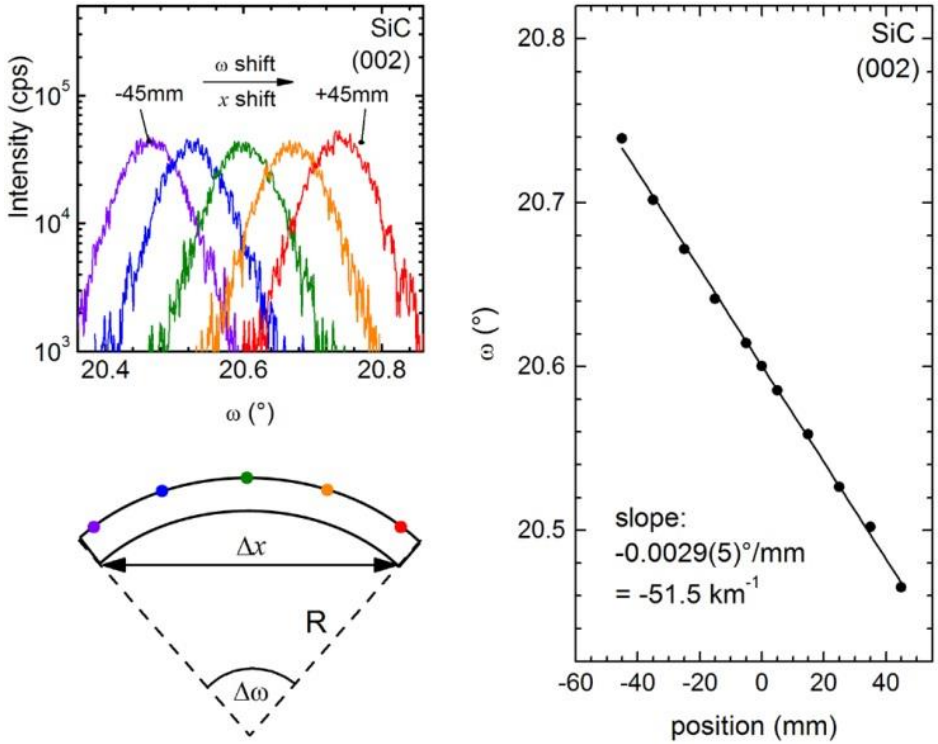

Wafer curvation κ:

$$\kappa = \frac{1}{R} = \frac{\tan(\Delta\omega)}{\Delta x} \approx \frac{\Delta\omega}{\Delta x}$$

M. Frentrup et al., J. Phys. D: Appl. Phys. **50** (2017) 433002

Reciprocal Space Mapping (RSM)

Reciprocal space Map

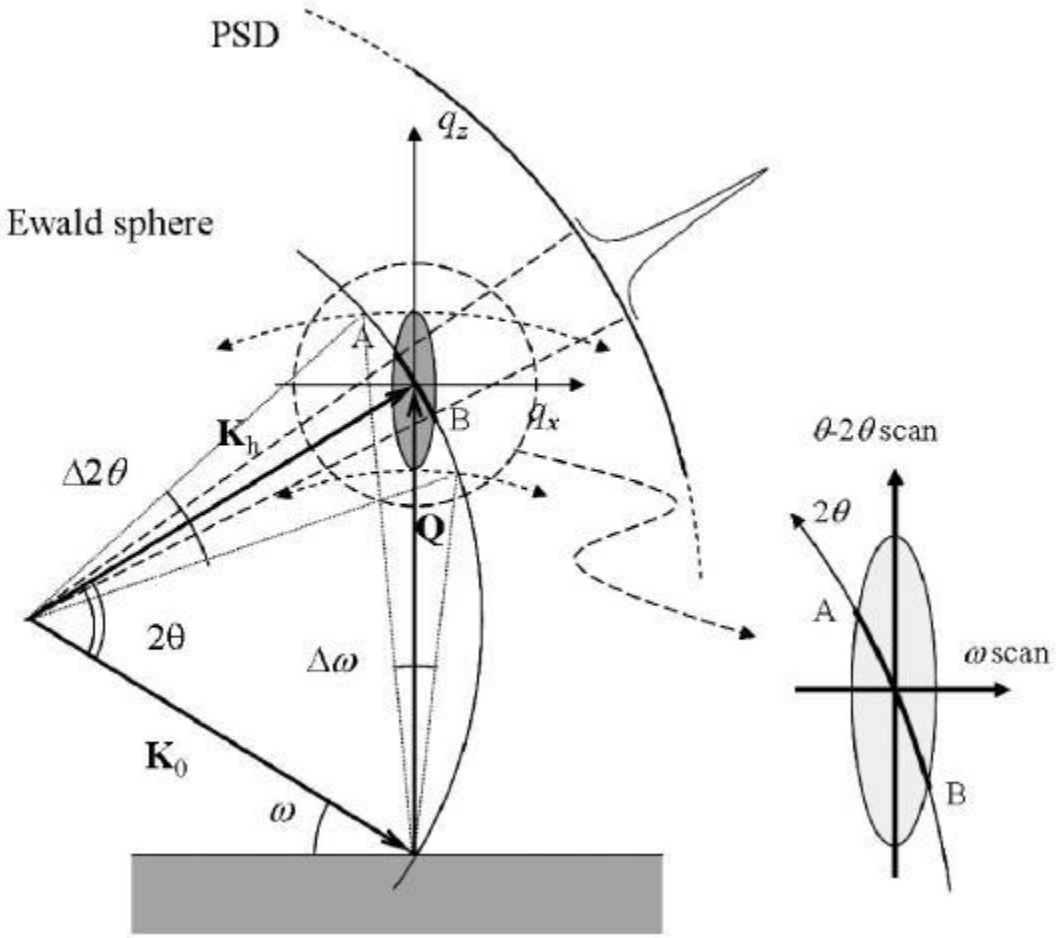

RSM of cubic GaN with and without hexagonal Inclusions

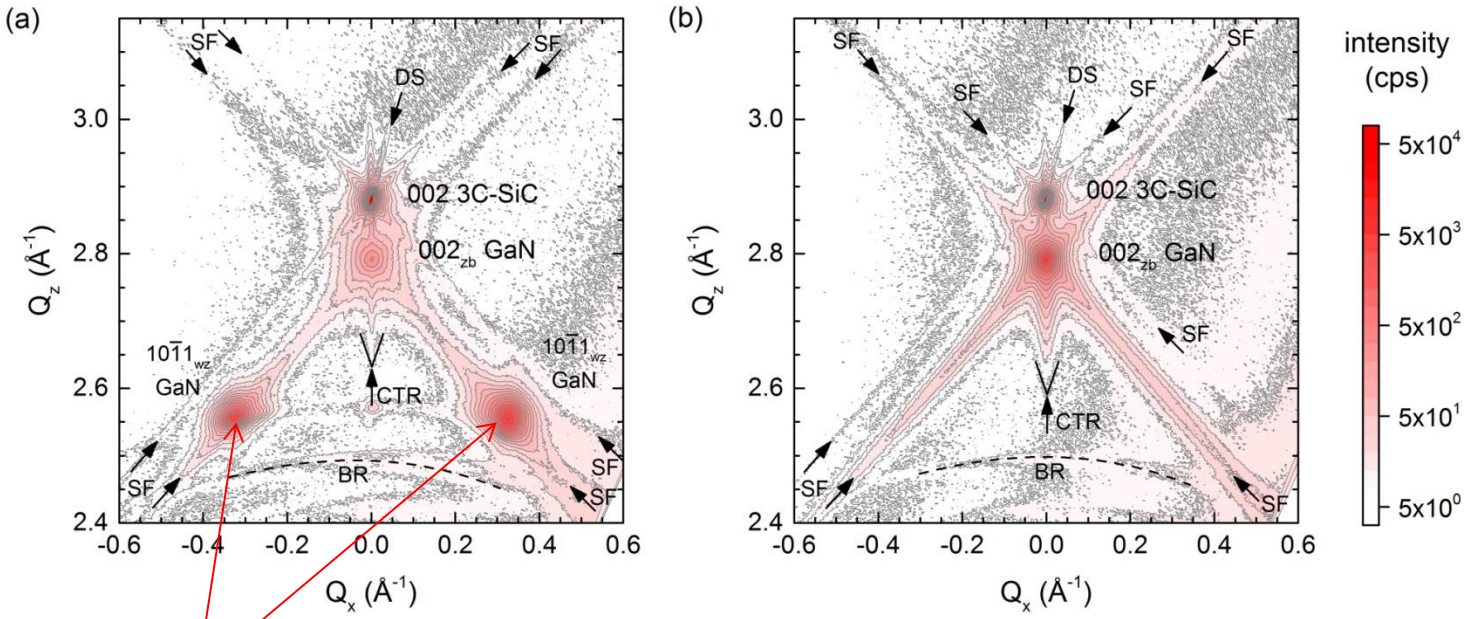

hex. inclusions

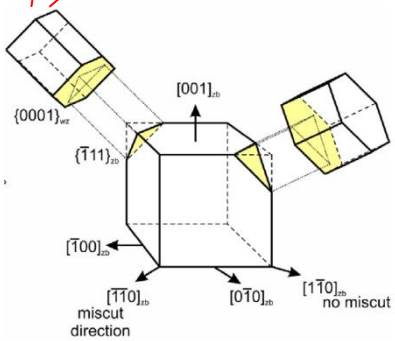

SF … stacking faults
DS … detector streaks
CTR .. Crystal truncation rod
BR … Bragg ring (from polycrystaline SiC)

k-space map

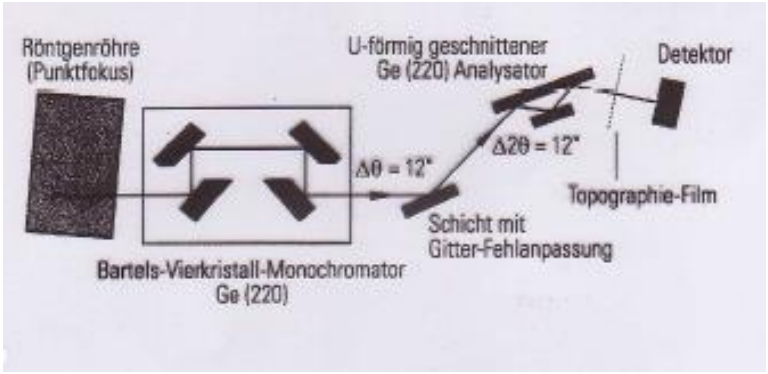
Röntgenröhre
(Punktfokus)
U-förmig geschnittener
Ge (220) Analysator
Detektor
Δθ = 12"
Δ2θ = 12"
Topographie-Film
Schicht mit
Gitter-Fehlanpassung
Bartels-Vierkristall-Monochromator
Ge (220)

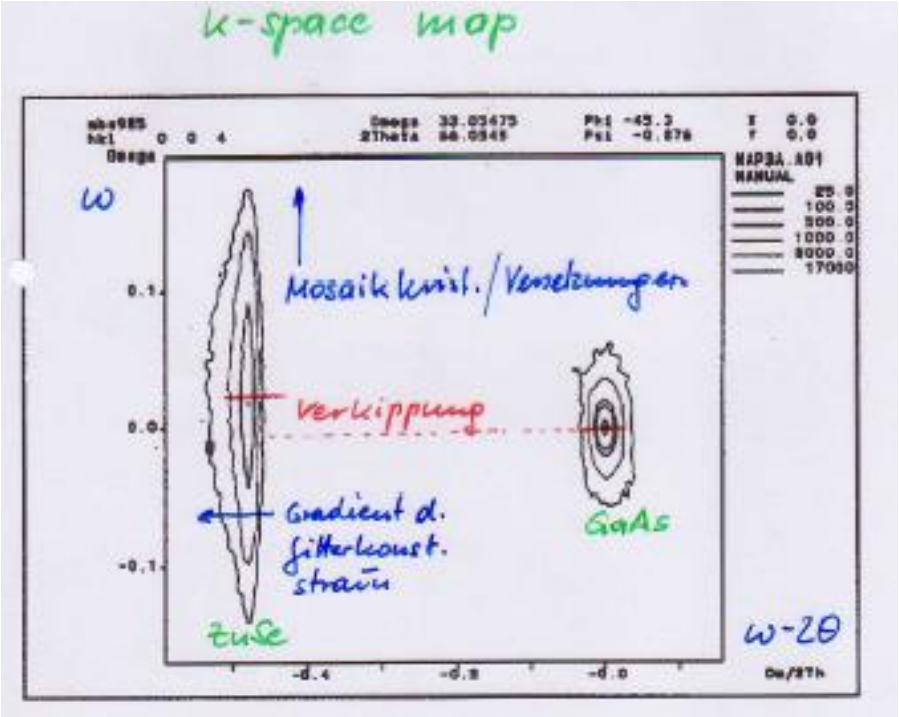
k-space map
ω
Mosaikkrist./Versetzungen
Verkippung
Gradient d.
Gitterkonst.
strain
GaAs
tuSe
ω-2θ

Glazing incident XRD (GIXRD)
X-ray Reflection (XRR)

Diffractometry of thin layers

Investigations of thin films with grazing incidence XRD

→ X-rays hit the lattice planes at the surface layer

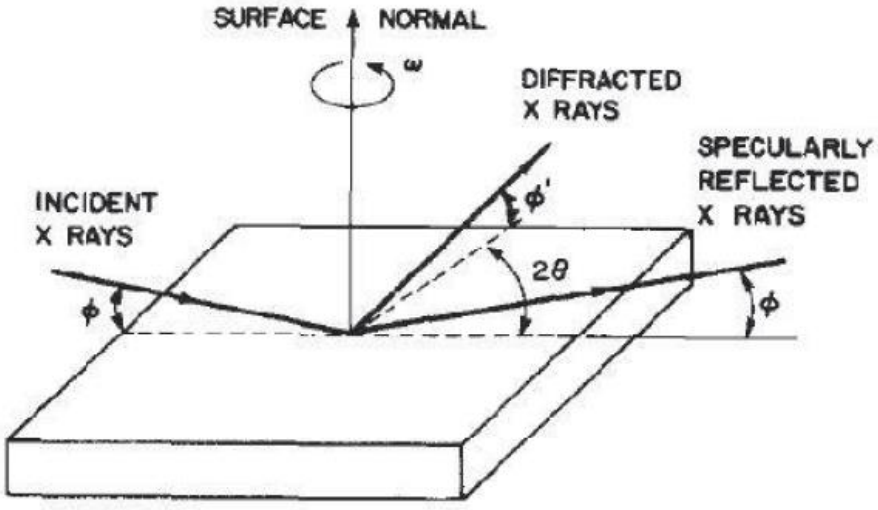

Schematic diagram of grazing-incidence x-ray diffraction (GID). θ Bragg angle, ϕ angle of incidence, ϕ' exit angle of diffracted beam, ω angle of rotation around surface normal (azimuth).

Angle of incidence typically < 4°, but larger than angle of total reflection
X-ray will be absorbed in the surface layer.

Angle smaller than angle of total reflection
diffraction of the evanescente wave (only a few surface monolayers)

X-ray reflection

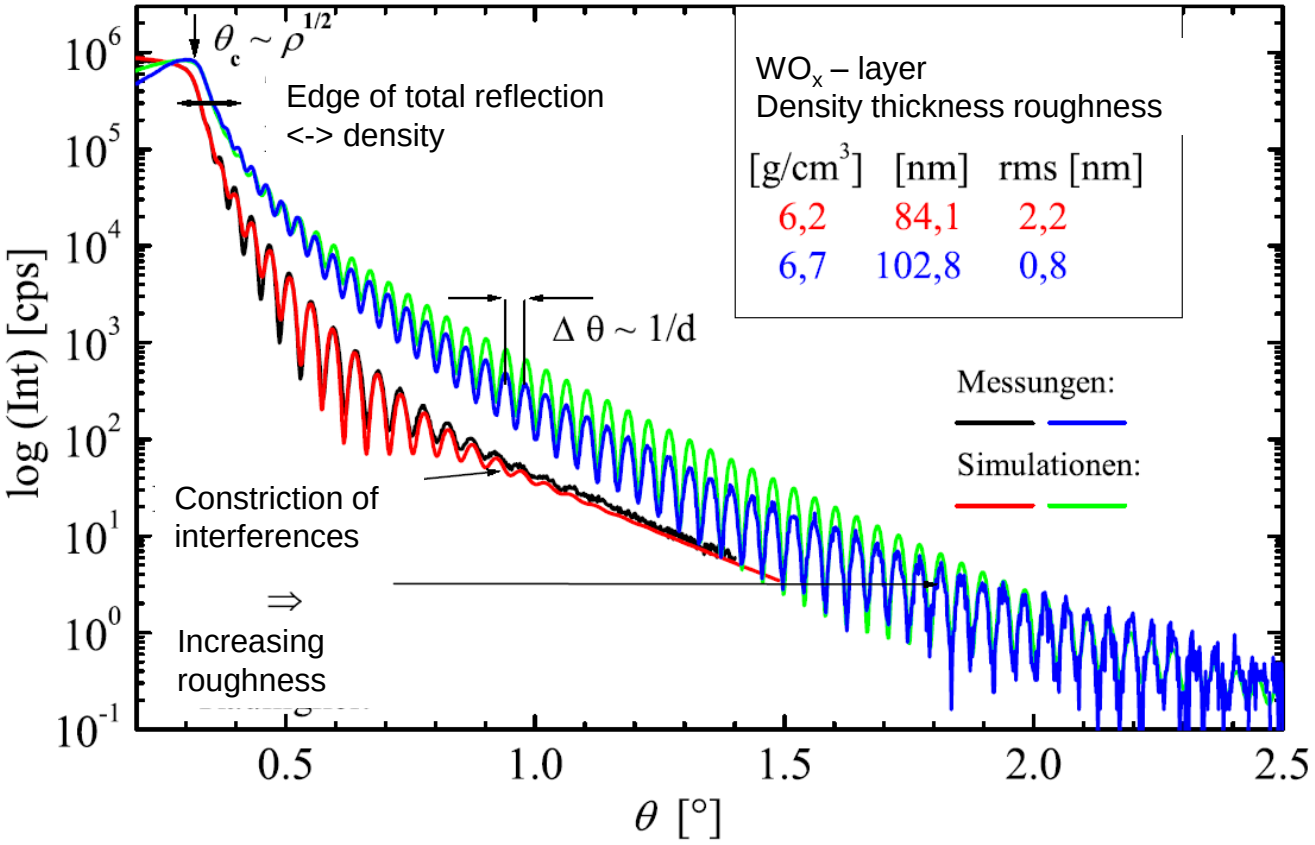

Film thickness d: $$d \approx \frac{\lambda}{2}\frac{1}{\sqrt{\theta_{m+1}^2-\theta_C^2}-\sqrt{\theta_m^2-\theta_C^2}} \approx \frac{\lambda}{2}\frac{1}{\theta_{m+1}-\theta_m}, \quad \text{f'ur } \theta_m \gg \theta_C.$$

Roughness ρ: $$\rho_{v,h}\cdot\exp\left(-\frac{d}{2\sigma^2}\right)$$

What techniques can be used to get which film information

	Thickness	Composition	Lattice Strain/ Relaxation	Defects	Orientation	Residual Stress	Crystallite Size
Perfect Epitaxy	XRR, HRXRD	HRXRD, RC	Assume 100%	Assume none	HRXRD	--	--
Nearly perfect epitaxy	XRR, HRXRD	HRXRD, RC	HRXRD	RC	HRXRD	--	--
Textured epitaxial*	XRR, HRXRD	HRXRD	HRXRD, IP-GIXD	RC	HRXRD	--	--
Strongly textured polycrystalline	XRR	XRPD, IP-GIXD	IP-GIXD	XRPD, IP-GIXD	IP-GIXD, PF	IP-GIXD	XRPD, IP-GIXD
Textured polycrystalline	XRR	XRPD, GIXD or IP-GIXD	--	XRPD, GIXD OR IP-GIXD	PF	Psi	XRPD, GIXD
Polycrystalline	XRR	XRPD, GIXD	--	XRPD, GIXD	PF	Psi	XRPD, GIXD
Amorphous	XRR	--	--	--	--	--	--

XRR- X-Ray Reflectivity
HRXRD- High Resolution XRD using coupled scan or RSM

RC- Rocking Curve
XRPD- Bragg-Brentano powder diffraction
GIXD- grazing incidence XRD

IP-GIXD- in-plane grazing incidence XRD
PF- pole figure
Psi- $\sin^2\psi$ using parellel beam

References

- P. Kidd , *XRD of gallium nitride and related compounds: Strain, composition and layer thickness*, PANalytical ISBN 978-90-809086-7-3
- M. Frentrup et al., J. Phys. D: Appl. Phys. **50,** 433002(2017)
- O. Masson et al., Rev. Sci. Instrum. **76**, 063912 (2005)
- S.A. Speakman, *Basics of X-ray Powder Diffraction*, MIT Center for Materials Science and Enginiering USA http://prism.mit.edu/xray
- S.A. Speakman, *Introduction to High Resolution X-Ray Diffraction of Epitaxial Thin films*, MIT Center for Materials Science and Enginiering, USA http://prism.mit.edu/xray
- M. Birkholz *Thin Film Analysis by X-ray Scattering*, Wiley-VCH (2006)
- P.F. Fewster *X-ray Scattering from Semiconductors*, Imperial College Press (2000)
- U. Pietsch , V. Holy, T. Baumbach, *High-Resolution X-ray Scattering from Thin Films to Lateral Nanostructures*, Springer (2004)

Thank you for your attention